ACTA GEOGRAPHICA SLOVENICA

GEOGRAFSKI ZBORNIK



2026
66
1

ACTA GEOGRAPHICA SLOVENICA
GEOGRAFSKI ZBORNIK
66-1 • 2026

Contents

Hasan BASRI, Tuti MUTIA, Abdul RASYAD, Ahmad TOHRI, Hanapi HANAPI, Muhamad ALI
The impacts of tourism on shifting mountain climbing ritual tradition in geopark Rinjani, Indonesia 7

Rok TURNIŠKI, Helena GRČMAN
Soils of the Dinaric karst in Slovenia: properties, pedogenesis and land use 21

Klemen COF, Uroš STEPIŠNIK, Manja ŽEBRE, Matej LIPAR
Hierarchical cluster classification and analysis of cirques in Slovenian Alps 39

Danijel DAVIDOVIĆ, Jure ČUŠ, Danijel IVAJNŠIČ
Land-use dynamics and grassland succession challenges in the Natura 2000 site Kras: The socioeconomic perspective 61

Zoltán BÁTORI, Kata FREI, Gábor LI, Orsolya VALKÓ, András VOJTKÓ, Csaba TÖLGYESI, Tünde FARKAS, Alida Anna HÁBENCZYUS, Ágnes TÓTH, László ERDŐS, Zsófia KRIVÁCS, Balázs DEÁK
Karstic microrefugia reflect diverse biogeographic affinities of vascular plant species 81

Boudjemline FOUZIA
Mapping and assessing forest fire severity using remote sensing indices: A case study of Tizi Ouzou, Algeria 99

Peter FRANTAR, Frank HERRMANN, Mišo ANDJELOV
National-scale water balance in Slovenia (1972–2024): Long-term trends and variability in water balance components 121

Juš GAŠPARIČ, Ana POTOČNIK BUHVALD, Dušan PETROVIČ
Satellite-based analysis of light pollution in Slovenia for the period 2013–2022 147

Entin HIDAYAH, Mokhammad Farid MARUF, Siti Norafida JUSOH, Joko WIDODO, Afif AMILUDDIN
Machine learning-based landslide susceptibility assessment for shallow landslide mitigation in the Gumitir Mountain Area, Indonesia 179

ISSN 1581-6613

ACTA GEOGRAPHICA SLOVENICA

66-1
2026

ISSN: 1581-6613 (*Print edition/tiskana izdaja*)
ISSN: 1581-8314 (*Online edition/spletna izdaja*)
UDC: 91
2026, ZRC SAZU, Geografski inštitut Antona Melika

International editorial board/mednarodni uredniški odbor: Zoltán Bátori (Hungary), David Bole (Slovenia), Marco Bontje (the Netherlands), Mateja Breg Valjavec (Slovenia), Michael Bründl (Switzerland), Rok Ciglič (Slovenia), Špela Čonč (Slovenia), Lóránt Dénes Dávid (Hungary), Mateja Ferk (Slovenia), Matej Gabrovec (Slovenia), Matjaž Geršič (Slovenia), Maruša Goluža (Slovenia), Mauro Hrvatin (Slovenia), Ioan Ianos (Romania), Peter Jordan (Austria), Drago Kladnik (Slovenia), Blaž Komac (Slovenia), Jani Kozina (Slovenia), Matej Lipar (Slovenia), Dénes Lóczy (Hungary), Simon McCarthy (United Kingdom), Slobodan B. Marković (Serbia), Janez Nared (Slovenia), Cecilia Pasquinelli (Italy), Drago Perko (Slovenia), Florentina Popescu (Romania), Garri Raagmaa (Estonia), Ivan Radevski (North Macedonia), Marjan Ravbar (Slovenia), Aleš Smrekar (Slovenia), Vanya Stamenova (Bulgaria), Annett Steinführer (Germany), Mateja Šmid Hribar (Slovenia), Jure Tičar (Slovenia), Jernej Tiran (Slovenia), Radislav Tošić (Bosnia and Herzegovina), Mimi Urbanc (Slovenia), Matija Zorn (Slovenia), Zbigniew Zwolinski (Poland)

Editors-in-Chief/glavna urednika: Rok Ciglič, Blaž Komac (ZRC SAZU, Slovenia)
Executive editor/odgovorni urednik: Drago Perko (ZRC SAZU, Slovenia)

Chief editors/področni urednik (ZRC SAZU, Slovenia):
- *physical geography/fizična geografija:* Mateja Ferk, Matej Lipar, Matija Zorn
- *human geography/humana geografija:* Jani Kozina, Mateja Šmid Hribar, Mimi Urbanc
- *regional geography/regionalna geografija:* Matej Gabrovec, Matjaž Geršič, Mauro Hrvatin
- *regional planning/regionalno planiranje:* David Bole, Maruša Goluža, Janez Nared
- *environmental protection/varstvo okolja:* Mateja Breg Valjavec, Aleš Smrekar, Jernej Tiran

Editorial assistants/uredniška pomočnika: Špela Čonč, Jernej Tiran (ZRC SAZU, Slovenia)
Journal editorial system manager/upravnik uredniškega sistema revije: Jure Tičar (ZRC SAZU, Slovenia)

Issued by/izdajatelj: Geografski inštitut Antona Melika ZRC SAZU
Published by/založnik: Založba ZRC
Co-published by/sozaložnik: Slovenska akademija znanosti in umetnosti

Address/naslov: Geografski inštitut Antona Melika ZRC SAZU, Gosposka ulica 13, p. p. 306, SI – 1000 Ljubljana, Slovenija; ags@zrc-sazu.si

The articles are available on-line/prispevki so dostopni na medmrežju: http://ags.zrc-sazu.si
This work is licensed under the/delo je dostopno pod pogoji: Creative Commons CC BY-SA 4.0

Ordering/naročanje: Založba ZRC, Novi trg 2, p. p. 306, SI – 1001 Ljubljana, Slovenija; zalozba@zrc-sazu.si

Annual subscription/letna naročnina: 20 €
Single issue/cena posamezne številke: 12 €

Cartography/kartografija: Geografski inštitut Antona Melika ZRC SAZU
Translations/prevodi: DEKS, d. o. o., Živa Malovrh
DTP/prelom: SYNCOMP, d. o. o.
Printed by/tiskarna: CICERO, Begunje, d. o. o.
Print run/naklada: 250 copies/izvodov

The journal is subsidized by the Slovenian Research and Innovation Agency (B6-7614) and is issued in the framework of the Geography of Slovenia core research programme (P6-0101)/Revija izhaja s podporo Javne agencije za znanstvenoraziskovalno in inovacijsko dejavnost Republike Slovenije (B6-7614) in nastaja v okviru raziskovalnega programa Geografija Slovenije (P6-0101).

The journal is indexed also in/revija je vključena tudi v: Clarivate Web of Science (SCIE – Science Citation Index Expanded; JCR – Journal Citation Report/Science Edition), Scopus, ERIH PLUS, GEOBASE Journals, Current geographical publications, EBSCOhost, Georef, FRANCIS, SJR (SCImago Journal & Country Rank), OCLC WorldCat, Google Scholar, CrossRef, and DOAJ.

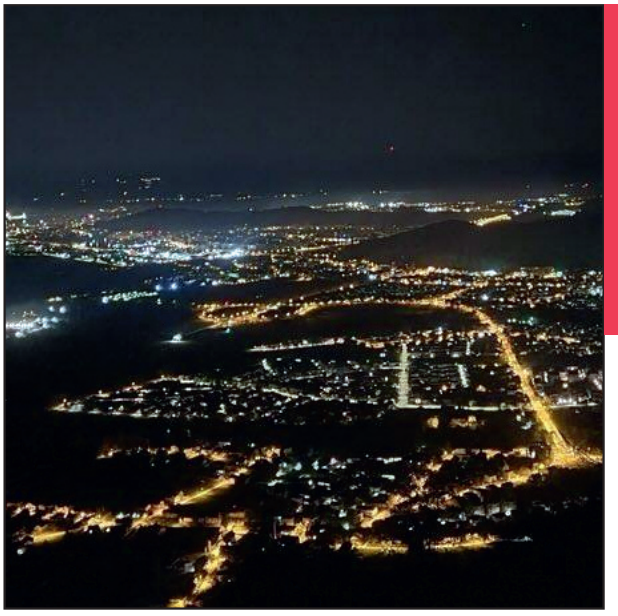
Design by/Oblikovanje: Matjaž Vipotnik

Front cover photography: Sečovlje Salt Pans at the Slovenian coast (photograph: SeanPavonePhoto, stock.adobe.com).
Fotografija na naslovnici: Sečoveljske soline na slovenski obali (fotografija: SeanPavonePhoto, stock.adobe.com).

Acta geographica Slovenica, 66-1, 2026, 147–177

SATELLITE-BASED ANALYSIS OF LIGHT POLLUTION IN SLOVENIA FOR THE PERIOD 2013–2022

Juš Gašparič, Ana Potočnik Buhvald, Dušan Petrovič



JUŠ GAŠPARIČ

Artificially illuminated night sky over Ljubljana.

DOI: https://doi.org/10.3986/AGS.14686
UDC: 504.6:628.9(497.4)"2013/2022"
Creative Commons CC BY-SA 4.0

Juš Gašparič[1], Ana Potočnik Buhvald[1], Dušan Petrovič[1]

Satellite-based analysis of light pollution in Slovenia for the period 2013–2022

ABSTRACT: Light pollution is a serious global issue that negatively affects human health, the environment, and wildlife, while also causing unnecessary energy consumption. Using satellite imagery from the S-NPP and NOAA-20 satellites, obtained via the Google Earth Engine platform, we analysed the situation in Slovenia from 2013 to 2022. Image processing involved inverse distance weighting interpolation and the kernel density estimation method. With time series we showed trends and ranges in the six major urban areas and with heat maps their spatial distribution. Special attention was given to the period of COVID-19 pandemic in 2020 by comparing the data with those from previous and subsequent years. The results revealed a slight overall increase in light pollution, consistent with global trends.

KEYWORDS: light pollution, spatial analysis, heat map, time series, VIIRS, Slovenian cities

Analiza svetlobnega onesnaženja v Sloveniji med letoma 2013 in 2022 na osnovi satelitskih posnetkov

POVZETEK: Svetlobno onesnaženje je resen globalni problem, ki negativno vpliva na zdravje ljudi, okolje in živali ter povzroča nepotrebno energetsko porabo. Z uporabo satelitskih posnetkov satelitov S-NPP in NOAA-20, pridobljenih prek platforme Google Earth Engine, smo analizirali stanje v Sloveniji med letoma 2013 in 2022. Posnetke smo obdelali z interpolacijo inverzne utežne razdalje in metodo ocene gostote jedra. S časovnimi vrstami smo prikazali trende in razpone na šestih večjih mestnih območjih, s kartami pojavnosti pa njihovo prostorsko razporeditev. Posebno pozornost smo namenili obdobju pandemije COVID-19 leta 2020 ter primerjali podatke z leti pred in po pandemiji. Rezultati kažejo rahlo splošno povečanje svetlobnega onesnaženja, kar je skladno z globalnimi trendi.

KLJUČNE BESEDE: svetlobno onesnaženje, prostorska analiza, karte pojavnosti, časovne vrste, VIIRS, slovenska mesta

The article was submitted for publication on August 4th, 2025.
Uredništvo je prejelo prispevek 4. avgusta 2025.

[1] University of Ljubljana, Faculty of Civil and Geodetic Engineering, Ljubljana, Slovenia

jus.gasparic97@gmail.com (https://orcid.org/0009-0009-3032-2530), ana.potocnik-buhvald@fgg.uni-lj.si (https://orcid.org/0000-0002-6662-1999), dusan.petrovic@fgg.uni-lj.si (https://orcid.org/0000-0001-5908-8180)

1 Introduction

According to the International Dark-Sky Association (IDA), light pollution encompasses the effects of artificial lighting and refers to the spread of artificial light into the environment, where it disrupts natural processes and functions. It originates mainly from improperly directed or overly intense sources such as streetlights, advertising billboards, illuminated buildings, and traffic lights (Chepesiuk 2009), and its increase is partly attributed to solid-state lighting (SSL), particularly light-emitting diodes (LEDs), which account for nearly 50% of global lighting sales (Barentine 2025). Light pollution is not only an environmental or astronomical issue but also a spatial and geographical phenomenon (Lamphar 2020), as it reflects the distribution of human activities, settlement structures, transport networks, and land-use patterns, and is closely linked to urbanisation and infrastructural development. Nighttime illumination therefore serves as an indirect indicator of social, economic, and spatial dynamics (Wu et al. 2023). Artificial light at night also disrupts circadian rhythms and contributes to energy waste and climate-related impacts (Brayley and Wakefield 2022; Garavito et al. 2023; Duan et al. 2024), although the present study focuses on its spatial and temporal dimensions.

Light pollution is analysed using ground-based and satellite measurements that differ in accuracy and spatial coverage. Common local instruments include Sky Quality Meters (SQM), digital cameras, and lux or luminance meters (Widmer et al. 2022). SQM values are expressed in magnitudes per square arcsecond (mag/arcsec^2), whereas other instruments measure illuminance (lux) or luminance (cd/m^2). Urban areas typically record 16–18 mag/arcsec^2, while darker sites reach around 22 mag/arcsec^2 or more (Žiberna and Gulič 2020). At the global scale, key datasets are provided by satellites operated by the National Oceanic and Atmospheric Administration (NOAA), particularly the Visible Infrared Imaging Radiometer Suite Day/Night Band (VIIRS DNB) sensor (Chen et al. 2021b), which enables long-term monitoring and visualisation of spatial and temporal changes. Analyses indicate that 83% of the global and 99% of the European population live under light-polluted skies (Falchi et al. 2016), and data from the Suomi National Polar-orbiting Partnership (S-NPP) satellite show a 2.2% annual global increase over the past decade (Kyba et al. 2023), while declines are rare and mainly associated with military conflicts (Li et al. 2018). In Central Europe, studies using VIIRS data report increasing radiance around major transport corridors, industrial zones, and expanding suburban areas in Austria, northern Italy, and Croatia (Widmer et al. 2022; Wallner et al. 2023).

In Slovenia, both approaches have been applied. Ground-based measurements include 48 locations near Maribor in 2012 (average 17.96 mag/arcsec^2), night skiing analyses at Rogla (20.20 mag/arcsec^2) and Mariborsko Pohorje (19.83 mag/arcsec^2) in 2018, and measurements in Gornja Radgona (17.25 mag/arcsec^2) and Senovo (17.87 mag/arcsec^2) in 2021 (Žiberna 2016; Žiberna and Gulič 2020; Kalšek et al. 2021). Several studies have also employed VIIRS data: Žiberna and Konečnik (2021) analysed distribution patterns by statistical regions, municipalities and Natura 2000 sites, while detailed analyses show that in 2017 the most illuminated municipalities were Ankaran (Luka Koper, 9.5 nW/cm^2/sr), Ljubljana (5.4 nW/cm^2/sr) and Maribor (4.8 nW/cm^2/sr) (Žiberna et al. 2018; Horvat et al. 2023). Radiance, expressed in nanowatts per square centimetre per steradian (nW/cm^2/sr), represents the luminous power emitted into the atmosphere and is a key indicator in remote sensing studies of nighttime illumination (LUC and Hoare 2024).

The aim of this study is to examine the extent of light pollution in Slovenia and its surroundings using satellite imagery from the NOAA VIIRS DNB sensor. Spatial patterns, differences, and trends are presented using heatmaps and multi-yeartime series. This approach provides a more detailed understanding of long-term illumination dynamics and allows us to assess the effects of extraordinary events such as the COVID-19 pandemic. The structure of the analysis is illustrated in Figure 1.

Based on these considerations, the study addresses the following research questions:

(1) How did light pollution levels change in six selected Slovenian urban areas between 2013 and 2022 (chapters 3.1 and 3.2)?
(2) What spatial patterns of nighttime illumination can be observed at the city (chapter 3.2) and national scale (chapter 3.4)?
(3) How did an exceptional event such as the COVID-19 pandemic influence radiance levels in the country's largest urban area (chapter 3.3)?

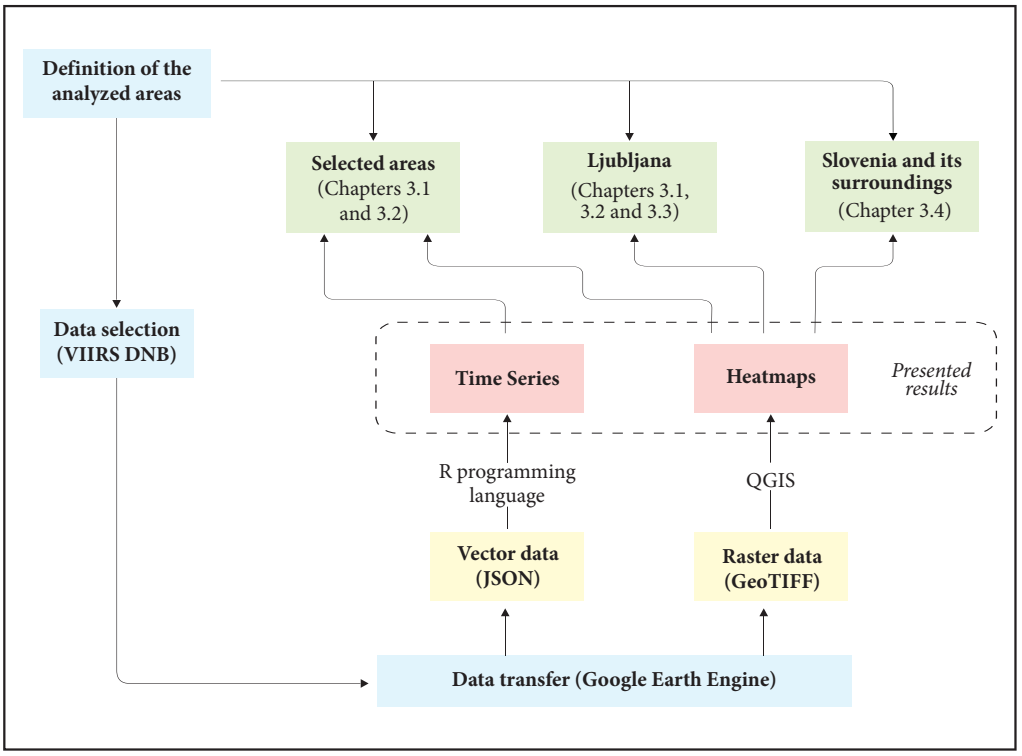


Figure 1: Analysis of Light Pollution in Slovenia flow chart.

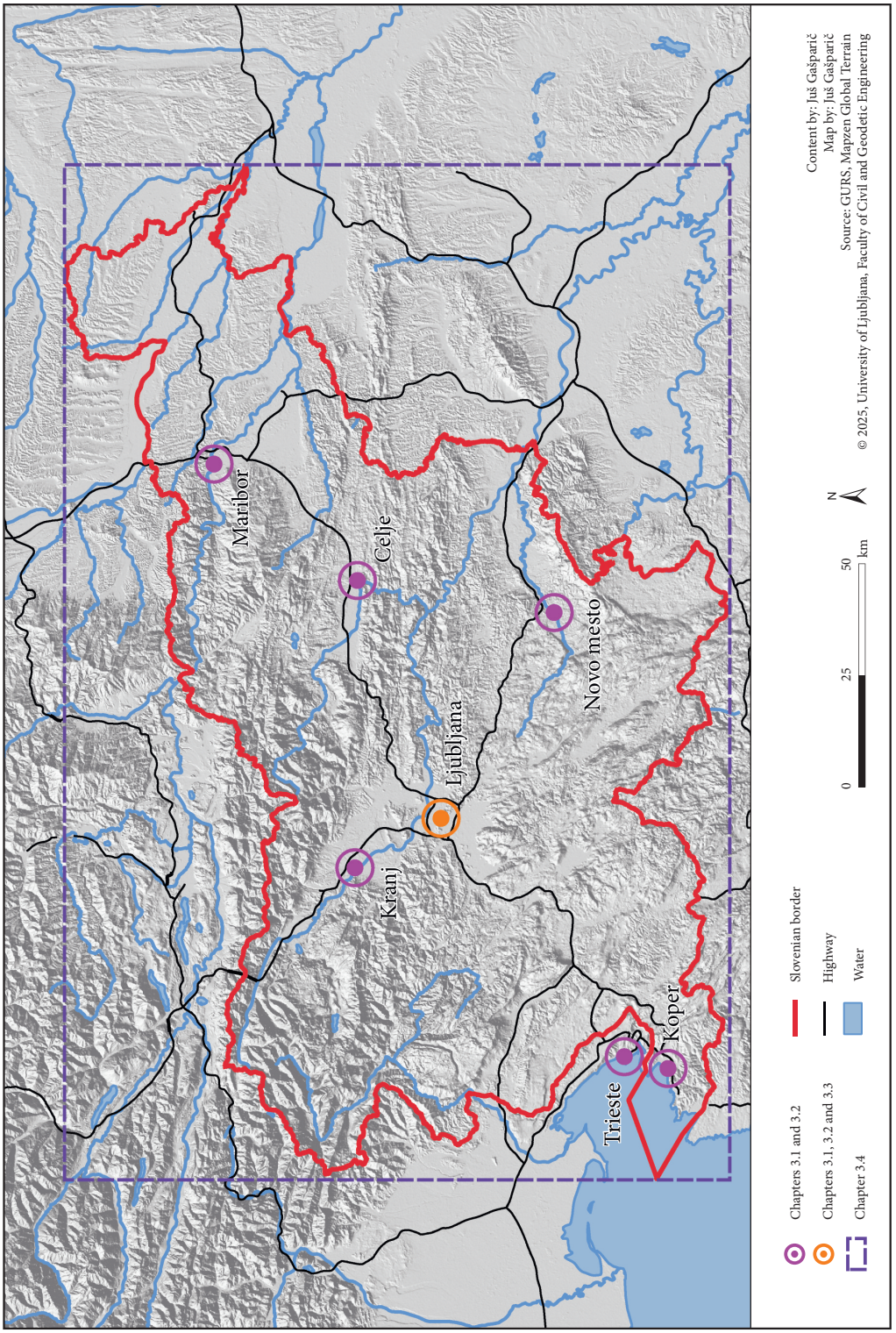
2 Methodology

2.1 Analysed area

Slovenia is a small but highly diverse country in terms of landscape and topography, commonly divided into Alpine, Pannonian, Dinaric and Mediterranean landscape types (Perko, Ciglič and Hrvatin 2021). As one of the most centralised countries in Europe, most political, economic and cultural activity is concentrated in Ljubljana (Vlaj 2012), while other major urban centres – Maribor, Celje, Kranj, Novo mesto and Koper – represent important regional, economic and employment centres, where investments, creative occupations, research activities and commuting flows are concentrated (Bole 2011; Ravbar 2011; Nared et al. 2017). The coastal cities of Koper and Trieste (Italy) form a cross-border port and logistics region of international relevance (Sessa 2021; Valinger Sluga and Ažman Momirski 2024). These spatial and economic characteristics shape patterns of nighttime illumination and provided the framework for analysing light pollution in three complementary components (Figure 2):

(1) Six major and economically important urban areas – Ljubljana, Maribor, Celje, Kranj, Novo mesto and the cross-border Koper–Trieste (Italy) region (with Novo mesto included instead of Velenje due to its strong industrial base and regional representation, and the Koper area extended to Trieste (Italy) because of their closely connected port and transport systems) (chapters 3.1 and 3.2).
(2) Focus on Ljubljana during COVID-19 pandemic (chapter 3.3).

Figure 2: Overview of the study areas and the three analytical components. ► p. 151


Maribor
Celje
Ljubljana
Kranj
Novo mesto
Trieste
Koper
Chapters 3.1 and 3.2
Chapters 3.1, 3.2 and 3.3
Chapter 3.4
Slovenian border
Highway
Water
0
25
50
km
N
Content by: Juš Gašparič
Map by: Juš Gašparič
Source: GURS, Mapzen Global Terrain
© 2025, University of Ljubljana, Faculty of Civil and Geodetic Engineering

(3) The entire Slovenian territory including adjoining parts of neighbouring countries (chapter 3.4), as light pollution extends beyond administrative borders.

To contextualise spatial differences in nighttime illumination, we compiled basic demographic, infrastructural and regional indicators for each analysed area (Table 1).

Table 1: Selected data of the analysed urban areas (data obtained by Infrastructure Agency of the Republic of Slovenia, Statistical Office of the Republic of Slovenia and Municipality of Trieste).

Indicator	Ljubljana	Trieste (Italy)	Koper	Maribor	Celje	Kranj	Novo mesto
Area [km^2]	257	84	303	148	95	151	236
Population (2013)	282,994	206,772	53,322	111,374	48,657	55,527	36,285
Population (2022)	293,218	200,603	53,462	113,004	48,679	56,639	37,615
Population (trend 2013–2022)	+3.5%	−3.0%	+0.3%	+1.5%	0.0%	+2.0%	+3.7%
Total road length (2022) [km]	1219.5	/	675.4	720.8	431.5	422.2	613.1
Composite electricity consumption intensity (2022) [kWh/resident and kWh/business entity]	28,999	/	32,030	28,271	45,507	42,177	68,051

2.2 Data used

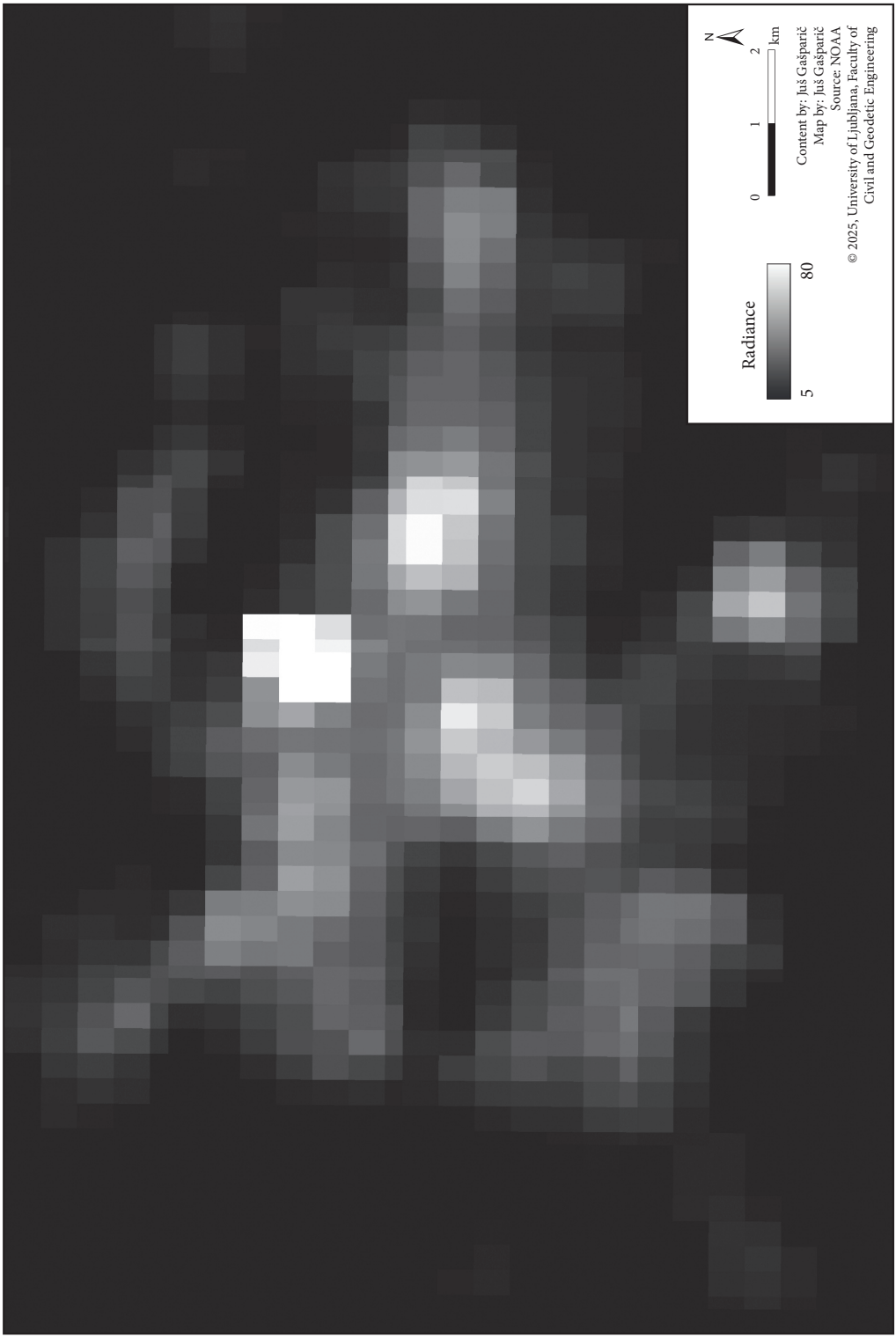
In this study, satellite data from the S-NPP and NOAA-20 satellites operated by NOAA and NASA were used. Both platforms carry five advanced instruments for high-resolution monitoring of the Earth's surface and climate (Keck 2011; Chen et al. 2020), including the VIIRS sensor, which acquires data in 22 spectral bands between 0.412 µm and 12.01 µm: 16 moderate-resolution bands, five high-resolution bands, and one panchromatic Day/Night Band (DNB). The DNB (0.5–0.9 µm) enables 24-hour observation with nearly constant 750 m spatial resolution across a 3,040 km swath and measures radiance over a wide dynamic range ($3.0 \times 10\text{-}9$ to $2.0 \times 10\text{-}2$ W/cm^2/sr) using calibrated detector arrays (Cao et al. 2013; Wolfe et al. 2013; Kolláth et al. 2018; Chen et al. 2021a; Wang et al. 2022). Nighttime light (NTL) data are recorded in radiance units (nW/cm^2/sr), suitable for detecting very weak light sources (Wang et al. 2022). Unlike the narrower spectral channels used for observing vegetation, ocean colour, clouds, and surface temperature, the DNB operates as a broad-band channel across the visible spectrum (Changyong et al. 2013) and supports monitoring of diverse nighttime light sources such as streetlights, building lighting, fishing vessels, gas flares, fires, auroras, and other human activities (Baynes 2024).

Monthly and annual NTL composites are generated from daily observations after removing atmospheric and lunar effects. Extreme values are excluded using a boxplot-based method based on the interquartile range (IQR = Q3 – Q1), omitting values outside Q1 – $1.5 \times$ IQR and Q3 + $1.5 \times$ IQR, this approach is robust and does not assume normal distribution. Final composites are calculated as the mean of the remaining observations, radiance values below 0.5 nW/cm^2/sr are set to zero to reduce background noise, and pixels affected by aurora are gap-filled with substitute values (Wang et al. 2022).

2.3 VIIRS Day/Night Band data and Google Earth Engine

We obtained the VIIRS Day/Night Band (DNB) data from the Google Earth Engine (GEE) Data Catalog. The analysis was based on annual composites from the datasets NOAA/VIIRS/DNB/ANNUAL_V21 (covering the period 2013–2021) and NOAA/VIIRS/DNB/ANNUAL V22 (for 2022). These datasets were developed and are maintained by the Earth Observation Group of the NOAA and National Centers for

Figure 3: NOAA VIIRS DNB ANNUAL 2022 maximum composite for the Ljubljana area, showing radiance values expressed in nanowatts per square centimetre per steradian (nW/cm^2/sr). ► p. 153


N
0
1
2
km
Radiance
5
80
Content by: Juš Gašparič
Map by: Juš Gašparič
Source: NOAA
© 2025, University of Ljubljana, Faculty of
Civil and Geodetic Engineering

Environmental Information (Elvidge et al. 2021). Although the 2022 data were obtained from the newer V22 product, both datasets represent annual VIIRS DNB night-time light composites produced within the same data framework and are therefore suitable for broad temporal comparison. Both datasets are publicly accessible via the GEE platform.These datasets contain yearly NTL composites expressed through various statistical indicators (median, average, maximum, and minimum), derived from cloud-free nighttime observations (Figure 3). In addition to these values, they include the total number of cloud-free observations for each pixel and the number of observations unaffected by sunlight or moonlight.

NTL data processing is based on monthly cloud-free averages. To remove extreme or irrelevant values caused by fires, auroras, and other sources of noise, the median radiance from the twelve-monthly composites is used. The background is filtered using a threshold determined by the data distribution across multiple years, enabling a consistent approach across the time series. The method also includes additional filters to reduce noise in polar regions, areas with high fire occurrence, and regions with low-intensity lighting such as rural settlements, diffuse glow from urban areas, and less illuminated surfaces (Elvidge et al. 2021). The processed VIIRS DNB data have a spatial resolution of 500 m (Widmer et al. 2022).

2.4 Data transfer

Raster and vector data were processed within the GEE environment using VIIRS DNB composites for the 2013–2022 period. Raster data in GeoTIFF format were extracted for predefined target areas defined by corner coordinates in the WGS84 coordinate system and subsequently exported from Google Earth Engine to Google Drive for further processing. These rasters contained annual radiance values and were subsequently imported into QGIS (version 3.36) for spatial visualisation and heatmap analysis. Vector data were derived from the same data catalogs after uploading manually delineated polygon layers representing the six urban areas selected for the first part of the study. The polygons encompassed zones with the highest radiance over built-up areas and were preferred to administrative municipal boundaries to ensure realistic inter-city comparisons, as municipal territories extend beyond urban cores and would otherwise lower average radiance values (Figure 4). GEE calculated annual minimum, mean, and maximum radiance statistics for each polygon, appending them as attributes to the geometries; each annual value represents the average of twelve-monthly composites (e.g., the maximum for Ljubljana in 2022 corresponds to the mean of that year's highest monthly values). The processed vector data were exported in JSON format and used to construct radiance time series for the six urban areas over 2013–2022.

2.5 Spatial analysis

Inverse Distance Weighted (IDW) interpolation is commonly used in spatial analyses to estimate unknown values based on known values from surrounding points. The method assumes that closer points have more influence than distant ones, which is achieved by assigning weights to the known data points according to their distance from the unknown location (Šumrada 2005). As distance increases, the weights decrease rapidly, with the rate of decrease controlled by the power value p (Barudžija et. al. 2024). When $p = 0$, all weights $_i$ are equal, resulting in a simple average of the neighbouring values. As p increases, the weights for distant points decrease more rapidly. At high p values, only the closest points significantly influence the interpolation (Equation 1).

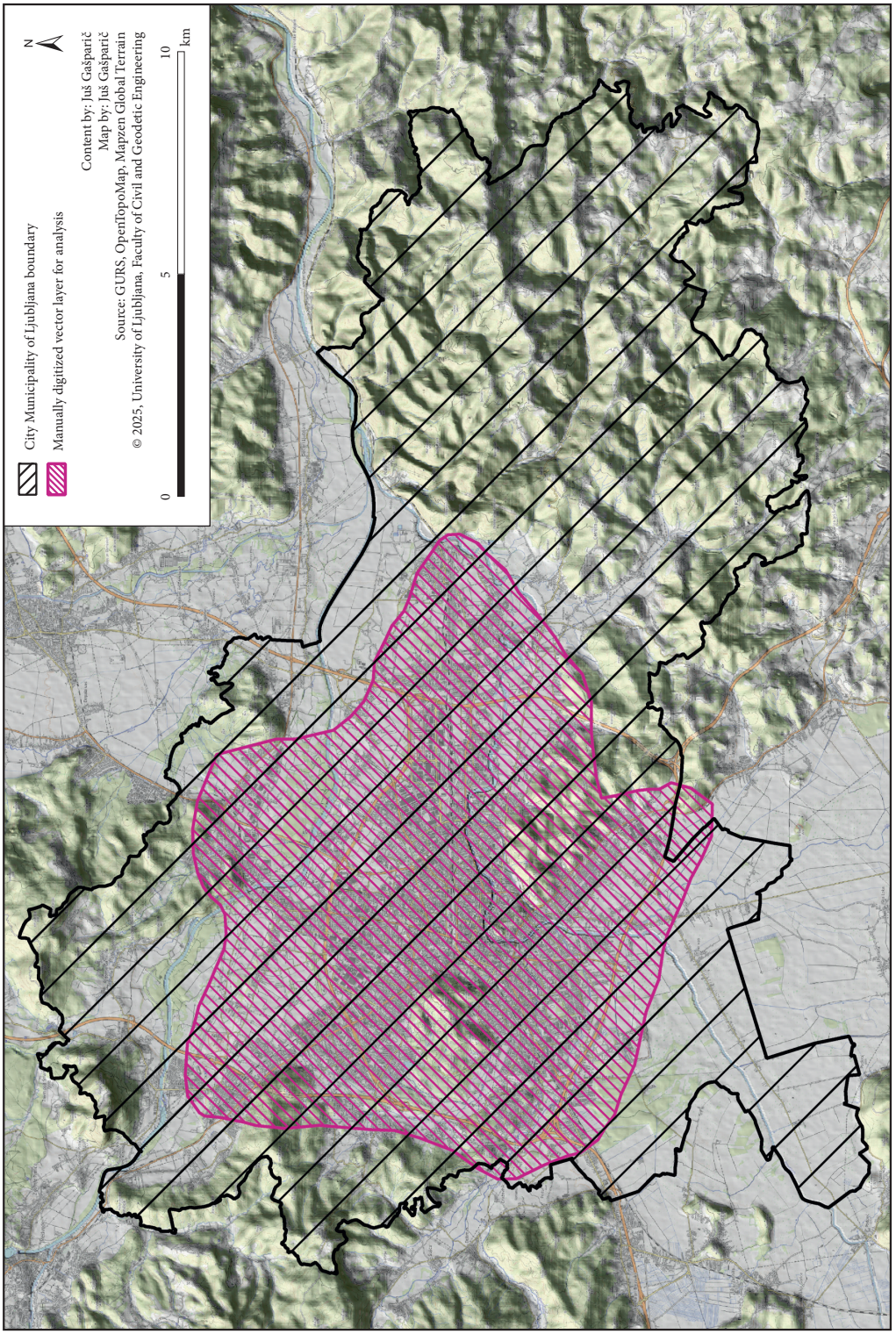
Mathematical expression IDW:

$$h_x(t_x) = \frac{\sum_{i=0}^{n} p_i(t_x,t_i) \cdot h_i}{\sum_{j=0}^{n} p_j(t_x,t_j)} \quad (1)$$

whereby

$$p_i(t_x, t_i) = \frac{1}{d_i(t_x, t_i)^k}$$

Figure 4: Comparison between the administrative area of the City Municipality of Ljubljana and the manually digitized area used for deriving radiance statistics. ► p. 155


City Municipality of Ljubljana boundary
Manually digitized vector layer for analysis
N
0
5
10
km
Content by: Juš Gašparič
Map by: Juš Gašparič
Source: GURS, OpenTopoMap, Mapzen Global Terrain
© 2025, University of Ljubljana, Faculty of Civil and Geodetic Engineering

and

$$d_i(t_x, t_i) = \sqrt{(x(t_x) - x(t_i))^2 + (y(t_x) - y(t_i))^2}$$

where:
- $h_x(t_x)$ is the interpolated value at point t_x,
- $h_i(t_i)$ is the given value at location t_i,
- p_i is a weight calculated based on distance,
- $d_i(t_x, t_i)$ is a distance between point and the known point t_i,
- k is a power that determines how quickly the influence of the point decreases with distance.

In practice, it is common to interpolate using the second power ($k = 2$), which means that the influence of the points decreases in inverse proportion to the square of the distance ($1/d^2$). The higher the potency, the faster the influence of distant points decreases (Benmoshe 2025). In our study, the points were the centroids of the pixels of the satellite images, which means that the points were uniformly distributed in space. In such a case, a reasonable choice is a weight value of k = 1, meaning that the influence of the points decreases inversely with distance ($1/d$). This moderate distance-decay function was selected to preserve broad spatial gradients in night-time light intensity while avoiding excessive local dominance of individual pixels. The interpolation distance was set to $d = 100$ m, which provides a fine output grid for visualisation while remaining consistent with the spatial resolution and positional uncertainty of the original VIIRS DNB observations. IDW interpolation was used to produce spatial NTL heatmaps of major urban centres in 2021 and of the City of Ljubljana during the COVID-19 pandemic (chapters 3.2 and 3.3).

Kernel Density Estimation (KDE) is a method for creating smooth density surfaces that show where data points are concentrated or sparse (Wang et al. 2020). It is especially useful for visualising spatial patterns, identifying so-called »hotspots«, and estimating distributions without assuming a specific shape (Milić et al. 2020). Instead of counting points within a defined area, KDE assigns each point a smooth kernel function, which spreads influence outward from the point. All kernels are then summed to generate a continuous density surface. The shape of the kernel determines how influence decays with distance, and the bandwidth (radius) defines the extent of this influence. A larger radius results in a smoother estimate (Equation 2).

Let $(x_1, x_2, \ldots, x_n)$ be independently and identically distributed samples drawn from some univariate distribution of unknown density f at any given point x. We are interested in estimating the shape of this function f. Its kernel density estimator is:

$$\hat{f}_h(x) = \frac{1}{n}\sum_{i=1}^{n} K_h(x - x_n) = \frac{1}{nh}\sum_{i=1}^{n} K\left(\frac{x - x_i}{h}\right) \quad (2)$$

where:
- $\hat{f}_h(x)$ is the estimated density at point x,
- n is the number of data points (sample size),
- $h > 0$ radius,
- x_i observed data point (sample value) from the dataset,
- $K(\cdot)$ is the kernel function.

For the shape of the kernel, we used the quartic (biweight) function $K(u)$, which is defined:

$$K(u) = \begin{cases} 15/16\ (1 - u^2)^2\,; & |u| \le 1 \\ 0\,; & |u| > 1 \end{cases}$$

In our analysis, KDE was applied to the centroids of pixels where radiance exceeded 20 nW/cm^2/sr to analyse their spatial distribution. Kyba et al. (2017) showed that most global artificial light emissions originate from regions with radiance values below this threshold, indicating that only the most intense sources exceed it, while Hügli (2021) used the same threshold to delineate highly illuminated urban areas. A radius of 5,000 m was chosen as a balance between spatial detail and interpretability. Using the default quartic kernel in QGIS (version 3.36), KDE produced a GeoTIFF raster in which pixel values represent estimated point density, with higher values indicating greater concentration. The result expresses density per unit area rather than absolute radiance, as in IDW; however, the term »radiance« was retained in the legend because the >20 nW/cm^2/sr threshold determined the output. KDE was used to visualise the spatial distribution of light pollution across Slovenia and its surroundings (chapter 3.4).

2.6 Heatmaps and time series

A heatmap is a cartographic technique used to display geospatial data using colour gradients. Different colour shades represent either the intensity of values (IDW interpolation) or the density of occurrences (KDE) within a specific area, a methodological approach similarly applied by Karpińska and Kunz (2019; 2023) to analyse spatial patterns and temporal variability of night-time sky brightness in urban environments. For visualising quantitative satellite data such as VIIRS, we used convergent and divergent colour scales. Areas with higher NTL values are represented using warm colours (e.g., red, orange), while cooler colours (e.g., green, blue) indicate lower intensities. The effectiveness of such cartographic choices in enhancing the readability and interpretability of light pollution maps has been demonstrated in previous studies (Kunz and Daab 2024). For the 2022 statistical visualisation, we used a monochromatic red palette, where more saturated tones reflect higher levels of light pollution. A key factor affecting the readability of heatmaps is the selection of an appropriate basemap, which provides spatial context and helps users better understand the locations being analysed. For visualisations, we used the Mapzen Global Terrain and OpenTopoMap as a basemap, while data from the Surveying and Mapping Authority of the Republic of Slovenia (GURS) were used to display the main roads, hydrological features, the national border, and the municipal boundary of Ljubljana. To overlay the raster analysis layer and the basemap effectively, transparency settings were adjusted to allow for simultaneous display with appropriate blending. However, care must be taken when combining colour-coded layers, as overlaying them can result in new colour tones. Users may misinterpret these as representing additional categories rather than a blend of two datasets. Such misinterpretations can lead to false conclusions, especially if mixed tones are perceived as separate classes.

Time series analysis allows for identifying trends and patterns over time. It enables us to track changes from year to year and relate them to environmental events. Additionally, time series can reveal cyclical patterns (if present) and allow for comparisons across multiple locations within the same timeframe which is crucial for understanding spatial disparities. In this study, time series graphs were essential for examining how light pollution levels evolved and what key factors influenced those changes (chapter 3.1). Data processing was conducted using R programming language (version 4.3.1). We created combined time series plots for all selected areas, standardising the y-axis radiance values (nW/cm^2/sr) across cities to enable easier comparison. Maximum, median, and minimum values of annual NTL composites were used as statistical indicators.

3 Results

3.1 Radiance analysis in major cities

Tables 2–7 show the raw annual radiance values obtained from manually delineated vector layers for each urban area. Alongside these values, the tables present the percentage change from the previous year, illustrating annual increases or decreases in radiance intensity. The time series graphs in Figure 5 show the evolution of minimum, maximum, and median radiance values between 2013 and 2022. Dark red points represent the median, while light red points represent the annual maximum and minimum radiance values. The lines connecting these points help visualise overall trends and variation in light pollution.

3.2 Spatial representation of NTL in major urban centres

The time series analysis reveals that the highest median levels of light pollution occurred in 2021. In that year, peak radiance values were recorded in Trieste (Italy) and Koper, Maribor, Celje (same level as in 2019), and Kranj (2018). In Novo mesto (2019) and Ljubljana (2017), the highest values were observed in earlier years, although the 2021 levels did not differ significantly. The heatmaps in Figures from 6 to 11 show the spatial distribution of light pollution in 2021, based on median VIIRS DNB composites.

Figure 5: Time series of radiance (nW/cm^2/sr) values in major urban centres between 2013 and 2022. ► p. 160
Figure 6: Spatial radiance (nW/cm^2/sr) distribution of light pollution in Ljubljana area. ► p. 161
Figure 7: Spatial radiance (nW/cm^2/sr) distribution of light pollution in Trieste (Italy) and Koper area. ► p. 162
Figure 8: Spatial radiance (nW/cm^2/sr) distribution of light pollution in Maribor area. ► p. 163
Figure 9: Spatial radiance (nW/cm^2/sr) distribution of light pollution in Celje area. ► p. 164
Figure 10: Spatial radiance (nW/cm^2/sr) distribution of light pollution in Novo mesto area. ► p. 165
Figure 11: Spatial radiance (nW/cm^2/sr) distribution of light pollution in Kranj area. ► p. 166

Table 2: Ljubljana: annual radiance statistics (nW/cm^2/sr) and change (%) compared to the previous year.

	minimum		mean		maximum	
	radiance	change	radiance	change	radiance	change
2013	6.83	/	10.79	/	28.11	/
2014	4.94	−27.7	13.13	21.7	21.34	−24.1
2015	8.54	72.9	12.96	−1.3	16.92	−20.7
2016	9.93	16.3	13.31	2.7	17.34	2.5
2017	9.03	−9.1	13.95	4.8	20.01	15.4
2018	9.55	5.8	13.57	−2.7	19.96	−0.2
2019	5.88	−38.4	13.55	−0.1	17.57	−12.0
2020	5.45	−7.3	12.71	−6.2	16.5	−6.1
2021	8.14	49.4	13.75	8.2	18.9	14.5
2022	8.08	−0.7	13.33	−3.1	19.9	5.3

Table 3: Trieste (Italy) and Koper: annual radiance statistics (nW/cm^2/sr) and change (%) compared to the previous year.

	minimum		mean		maximum	
	radiance	change	radiance	change	radiance	change
2013	10.23	/	15.8	/	23.93	/
2014	10.11	−1.2	16.32	3.3	22.81	−4.7
2015	10.91	7.9	15.44	−5.4	21.21	−7.0
2016	10.87	−0.4	15.64	1.3	21.07	−0.7
2017	11.14	2.5	16.29	4.2	20.78	−1.4
2018	11.79	5.8	15.7	−3.6	21.5	3.5
2019	12.05	2.2	15.9	1.3	20.97	−2.5
2020	11.25	−6.6	15.47	−2.7	20.28	−3.3
2021	12.19	8.4	16.34	5.6	21.49	6.0
2022	9.51	−22.0	15.6	−4.5	22.11	2.9

Table 4: Maribor: annual radiance statistics (nW/cm^2/sr) and change (%) compared to the previous year.

	minimum		mean		maximum	
	radiance	change	radiance	change	radiance	change
2013	7.74	/	14.05	/	19.83	/
2014	10.45	35.0	14.32	1.9	23.41	18.1
2015	9.91	−5.2	13.67	−4.5	17.4	−25.7
2016	10.83	9.3	15.01	9.8	22.69	30.4
2017	10.91	0.7	15.14	0.9	23.61	4.1
2018	11.68	7.1	14.83	−2.0	21.07	−10.8
2019	9.2	−21.2	15.02	1.3	19.35	−8.2
2020	7.36	−20.0	14.45	−3.8	18.14	−6.3
2021	12.54	70.4	16.27	12.6	25.15	38.6
2022	10.46	−16.6	15.51	−4.7	20.77	−17.4

Table 5: Celje: annual radiance statistics (nW/cm^2/sr) and change (%) compared to the previous year.

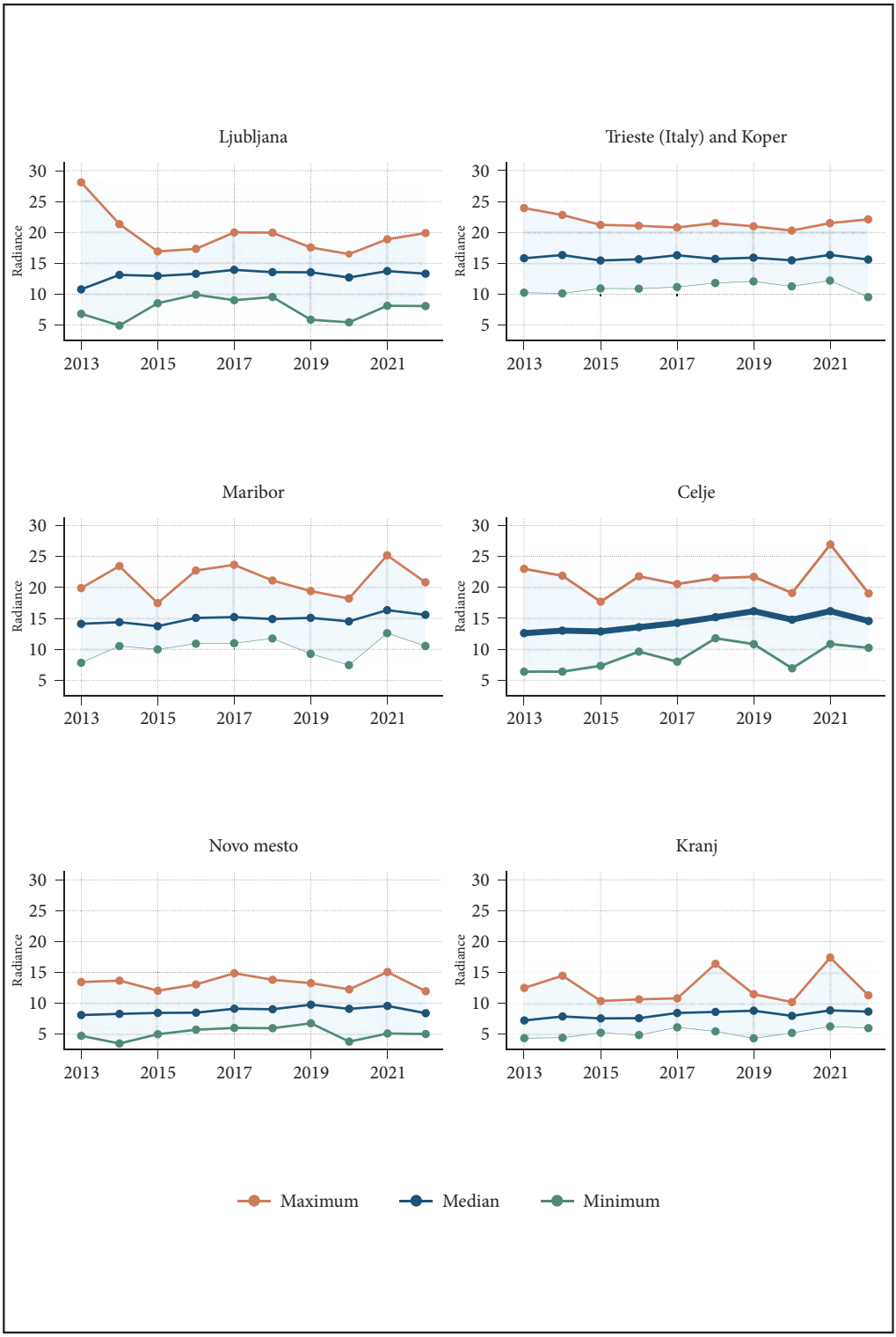
	minimum		mean		maximum	
	radiance	change	radiance	change	radiance	change
2013	6.39	/	12.61	/	23.02	/
2014	6.39	0.0	13.03	3.3	21.9	−4.9
2015	7.34	14.9	12.89	−1.1	17.7	−19.2
2016	9.63	31.2	13.58	5.4	21.81	23.2
2017	8.00	−16.9	14.26	5.0	20.56	−5.7
2018	11.79	47.4	15.19	6.5	21.53	4.7
2019	10.84	−8.1	16.17	6.5	21.72	0.9
2020	6.93	−36.1	14.8	−8.5	19.11	−12.0
2021	10.86	56.7	16.17	9.3	26.97	41.1
2022	10.24	−5.7	14.58	−9.8	19.04	−29.4

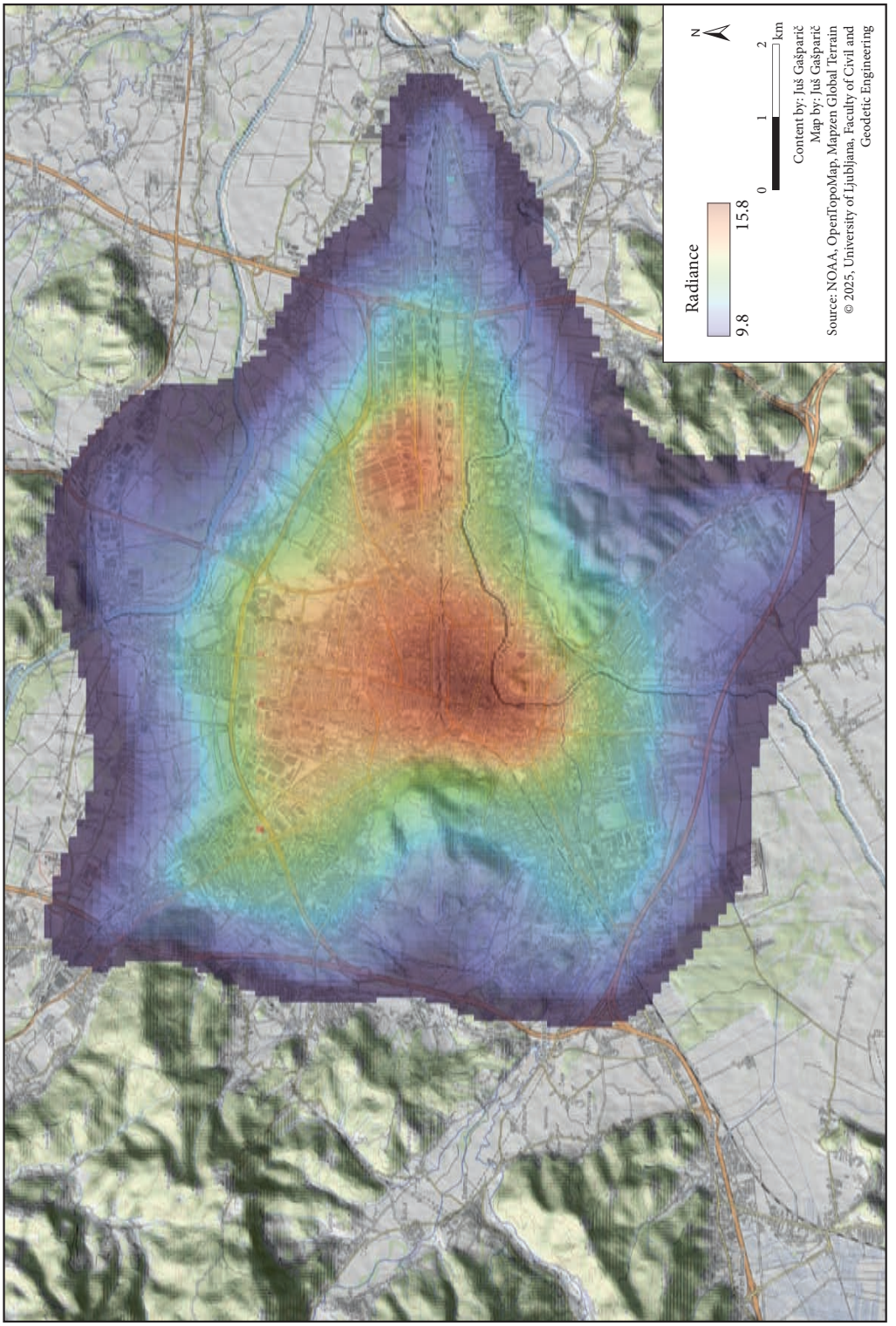
Table 6: Novo mesto: annual radiance statistics (nW/cm^2/sr) and change (%) compared to the previous year.

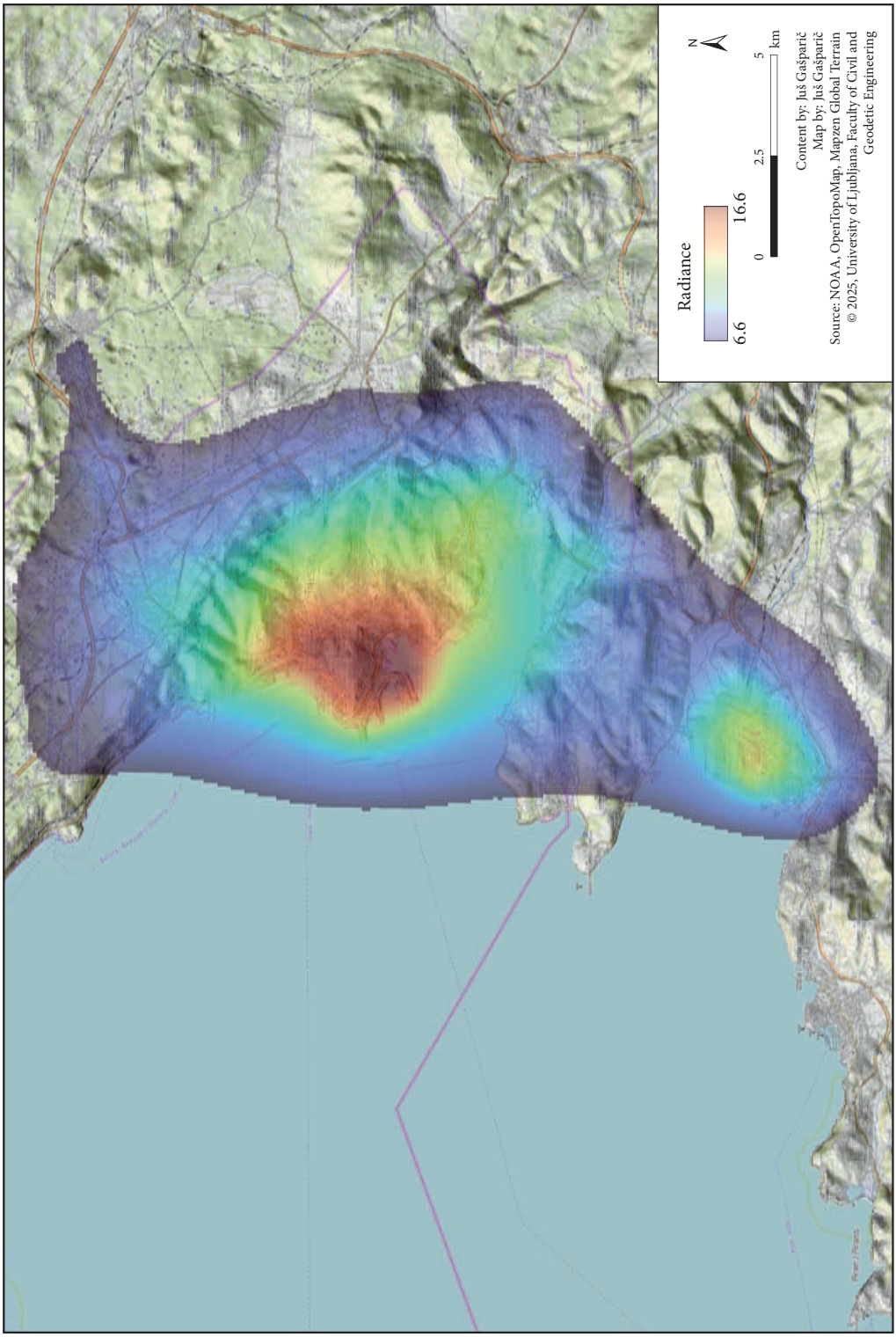
	minimum		mean		maximum	
	radiance	change	radiance	change	radiance	change
2013	4.78	/	8.14	/	13.48	/
2014	3.53	−26.2	8.32	2.2	13.70	1.6
2015	5.04	42.8	8.49	2.0	12.08	−11.8
2016	5.76	14.3	8.52	0.4	13.09	8.4
2017	6.05	5.0	9.16	7.5	14.90	13.8
2018	6.01	−0.7	9.07	−1.0	13.84	−7.1
2019	6.81	13.3	9.81	8.2	13.30	−3.9
2020	3.84	−43.6	9.14	−6.8	12.29	−7.6
2021	5.15	34.1	9.61	5.1	15.11	22.9
2022	5.07	−1.6	8.44	−12.2	12.00	−20.6

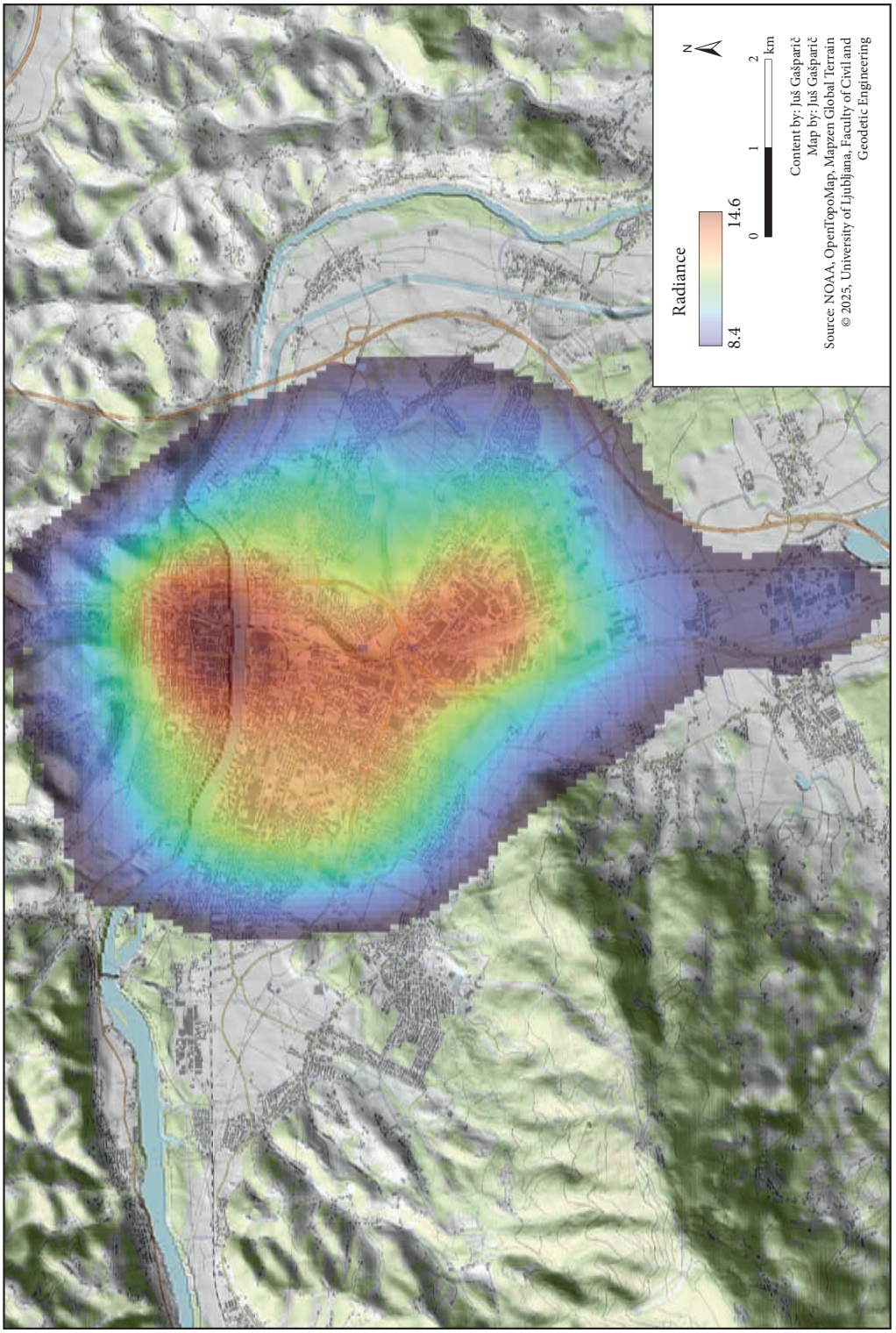
Table 7: Kranj: annual radiance statistics (nW/cm^2/sr) and change (%) compared to the previous year.

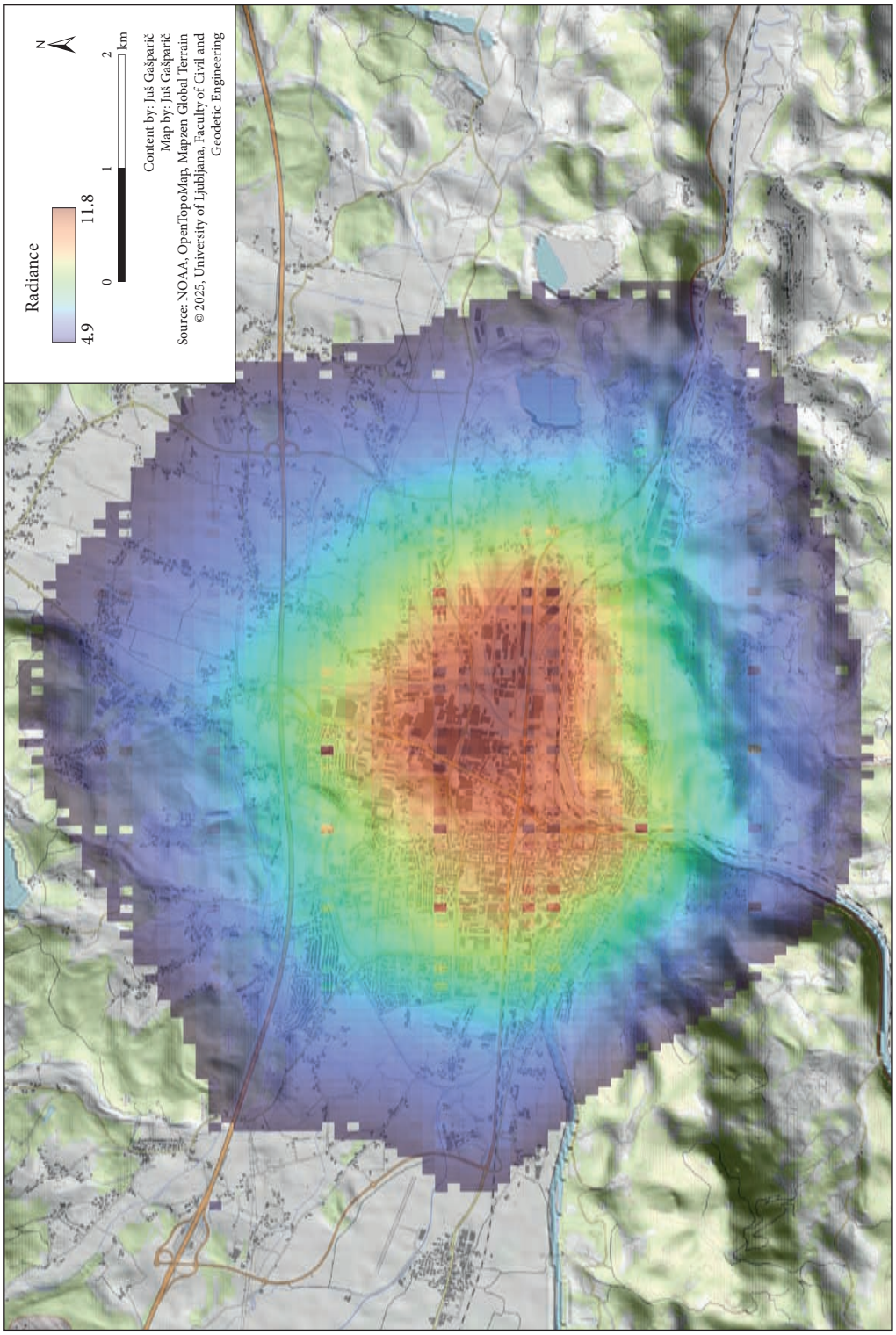
	minimum		mean		maximum	
	radiance	change	radiance	change	radiance	change
2013	4.35	/	7.23	/	12.49	/
2014	4.43	1.8	7.87	8.9	14.47	15.9
2015	5.23	18.1	7.55	−4.1	10.37	−28.3
2016	4.86	−7.1	7.59	0.5	10.64	2.6
2017	6.11	25.7	8.44	11.2	10.8	1.5
2018	5.45	−10.8	8.60	1.9	16.4	51.9
2019	4.33	−20.6	8.80	2.3	11.48	−30.0
2020	5.2	20.1	7.96	−9.5	10.19	−11.2
2021	6.25	20.2	8.85	11.2	17.41	70.9
2022	5.98	−4.3	8.65	−2.3	11.29	−35.2

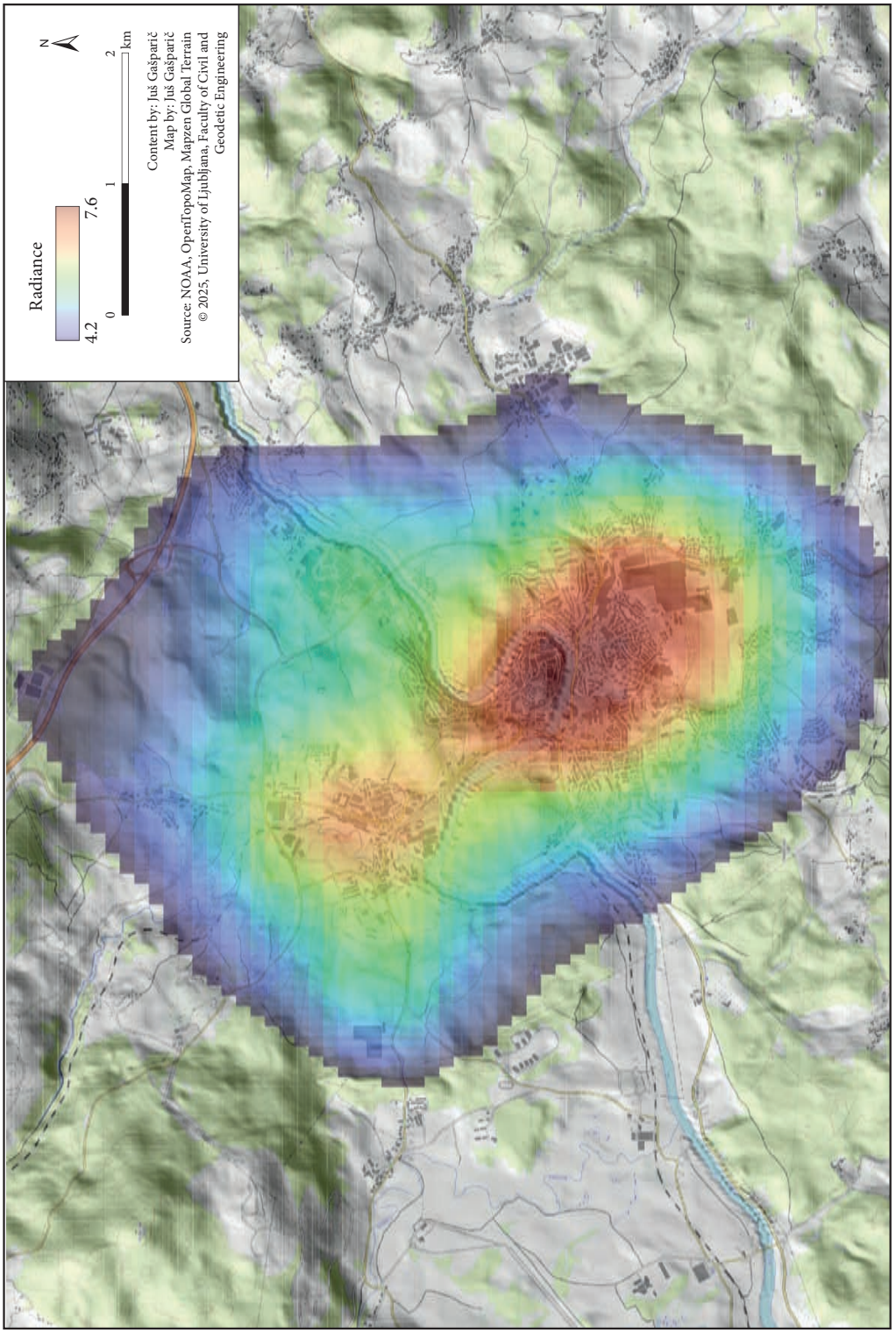

Ljubljana
Trieste (Italy) and Koper
Maribor
Celje
Novo mesto
Kranj
Radiance
30
25
20
15
10
5
2013
2015
2017
2019
2021
Maximum
Median
Minimum

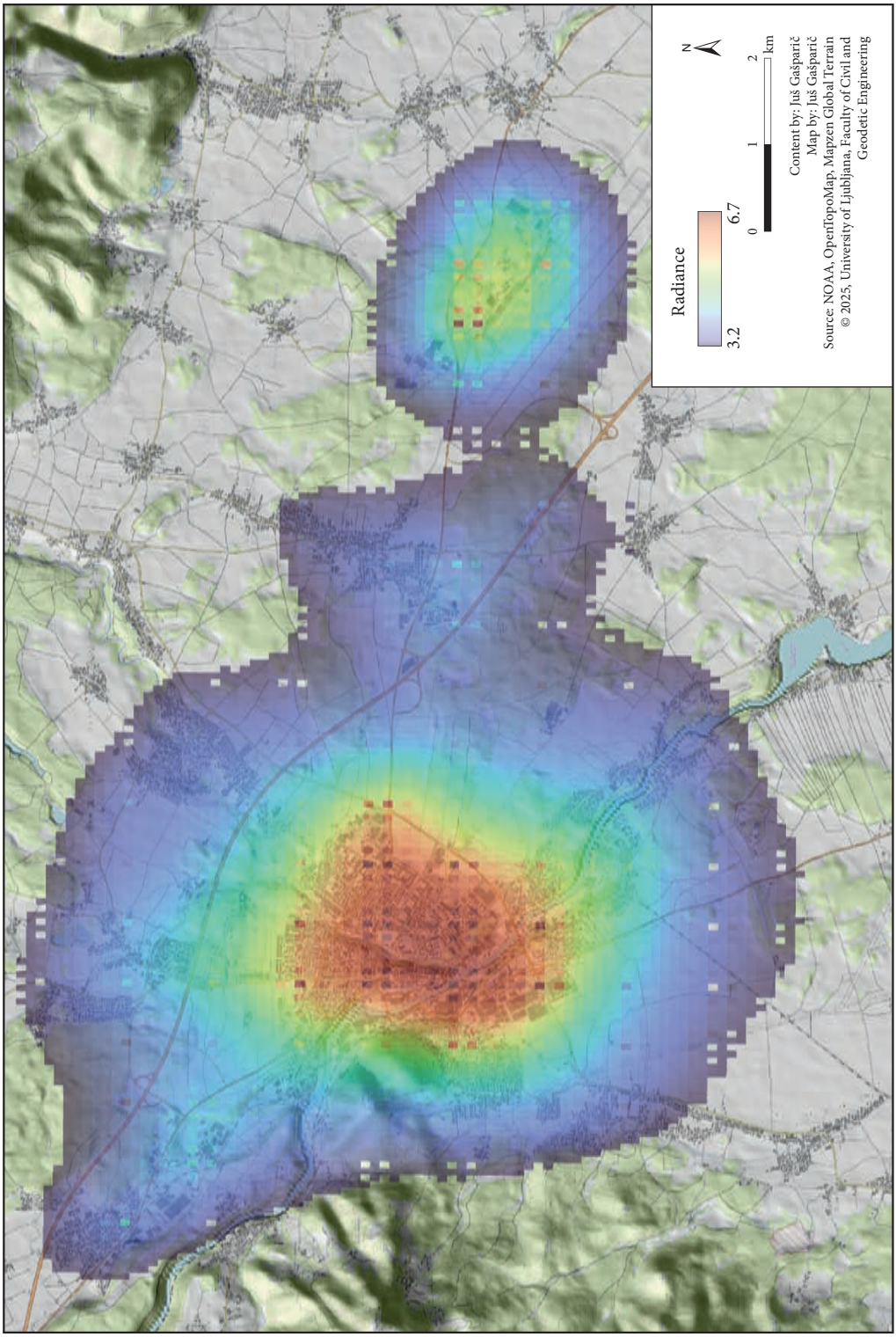

Radiance
9.8
15.8
N
0
1
2
km
Content by: Juš Gašparič
Map by: Juš Gašparič
Source: NOAA, OpenTopoMap, Mapzen Global Terrain
© 2025, University of Ljubljana, Faculty of Civil and Geodetic Engineering


N
Radiance
16.6
6.6
0
2.5
5
km
Content by: Juš Gašparič
Map by: Juš Gašparič
Source: NOAA, OpenTopoMap, Mapzen Global Terrain
© 2025, University of Ljubljana, Faculty of Civil and Geodetic Engineering


Radiance
14.6
8.4
N
0
1
2
km
Content by: Iuš Gašparič
Map by: Iuš Gašparič
Source: NOAA, OpenTopoMap, Mapzen Global Terrain
© 2025, University of Ljubljana, Faculty of Civil and Geodetic Engineering


Radiance
4.9
11.8
0
1
2
km
N
Content by: Juš Gašparič
Map by: Juš Gašparič
Source: NOAA, OpenTopoMap, Mapzen Global Terrain
© 2025, University of Ljubljana, Faculty of Civil and Geodetic Engineering


Radiance
4.2
7.6
0
1
2
km
N
Content by: Juš Gašparič
Map by: Juš Gašparič
Source: NOAA, OpenTopoMap, Mapzen Global Terrain
© 2025, University of Ljubljana, Faculty of Civil and Geodetic Engineering


Radiance
3.2
6.7
0
1
2
km
N
Content by: Juš Gašparič
Map by: Juš Gašparič
Source: NOAA, OpenTopoMap, Mapzen Global Terrain
© 2025, University of Ljubljana, Faculty of Civil and Geodetic Engineering

3.3 Difference in NTL before and after the COVID-19 pandemic in Ljubljana

This section presents absolute differences in NTL in Ljubljana between 2019 and 2020, and between 2020 and 2021 (Figures 12 and 13). The goal is to examine the effects of COVID-19 pandemic containment measures on light pollution levels, as visualised through comparative heatmaps. Analysis was conducted based on the maximum values of annual VIIRS DNB composites.The colour transitions on the maps are discrete, meaning attribute values are divided into classes, making boundaries between them more distinct. This visualisation enhances spatial interpretation and helps identify the main sources of light pollution. In the 2019–2020 comparison, the minimum visualised radiance difference is 1.0 nW/cm^2/sr, while in the 2020–2021 comparison, it is 2.0 nW/cm^2/sr. This difference (1.0–2.0) is necessary because there was a 6.1% decrease in 2020, followed by a 14.5% increase in 2021 (Table 2).

3.4 Minimum, average and maximum NTL values across Slovenia and its surroundings

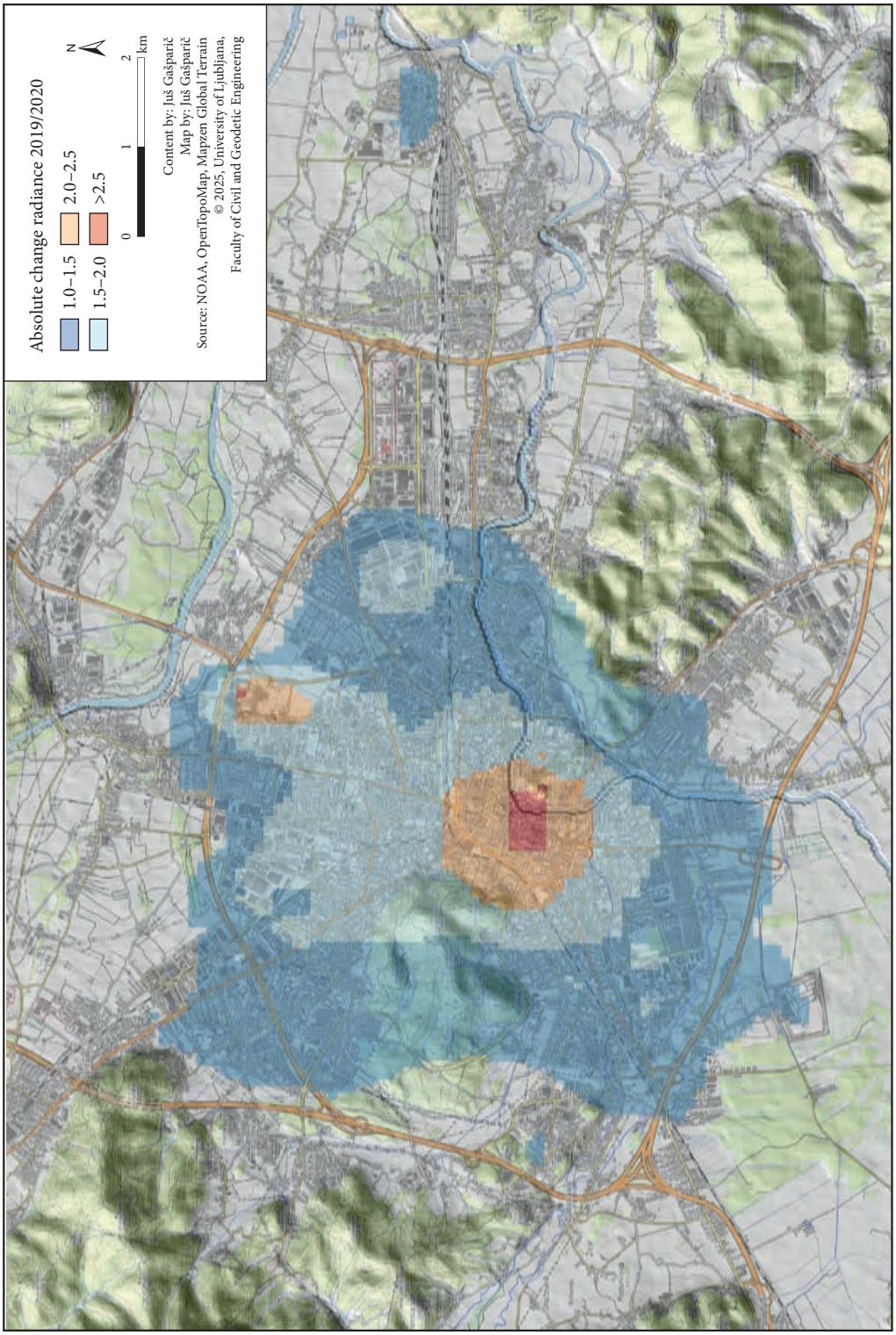
The time series graphs presented earlier revealed clear differences among the annual NTL composite statistics (minimum, median, and maximum radiance). To broaden the scope of the analysis, the spatial coverage was extended to encompass the entire territory of Slovenia and its wider surroundings, while the median statistic was replaced with the mean value. The resulting heatmaps visualize only those areas where radiance values exceeded 20 nW/cm^2/sr in 2022 as this threshold highlights the most intensely illuminated urban cores and allows for clearer differentiation from moderately or weakly lit surroundings (Figures from 14 to 16).

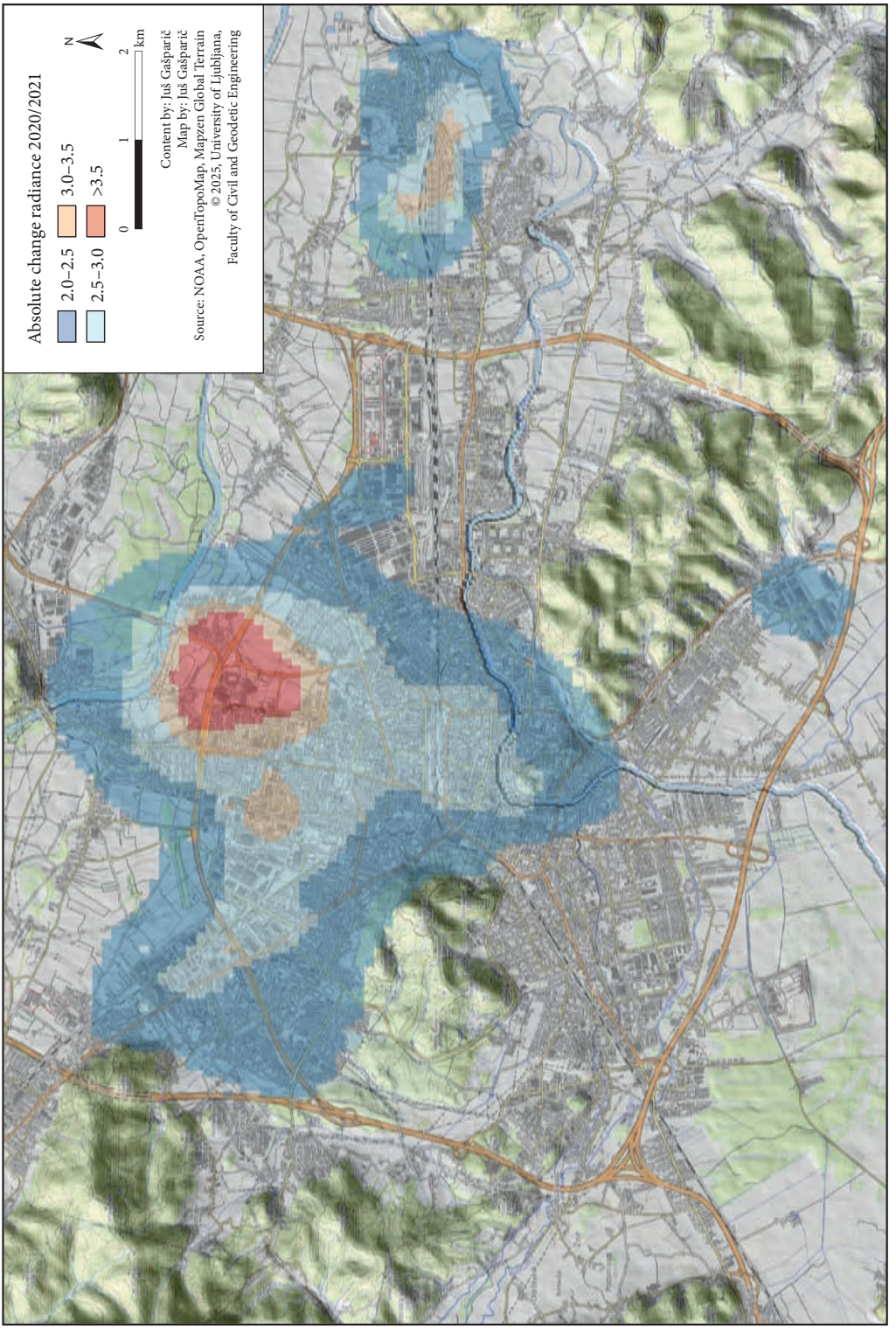
4 Discussion

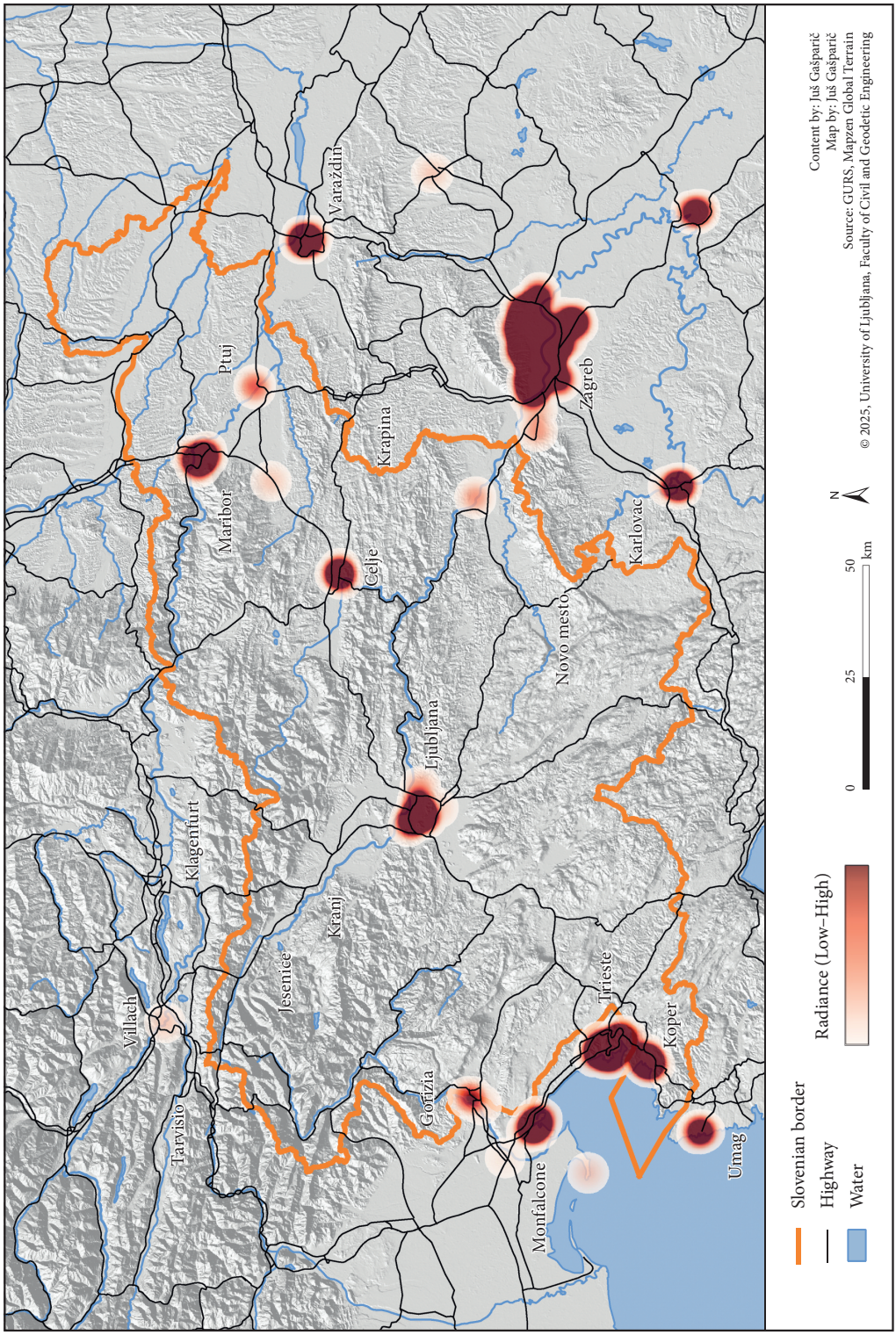
Tables 2–7 and time series (Figure 5) for six urban regions in Slovenia, including crossborder Trieste (Italy)–Koper area, from 2013 to 2022 present annual NTL radiance statistics. In Ljubljana, the mean radiance started at 10.8 nW/cm^2/sr in 2013, increased by +21.7% in 2014, and then fluctuated moderately between 12.7 and 13.9 nW/cm^2/sr through 2022 (−3.1% in the final year). The minimum values ranged between 6.8 and 9.9 nW/cm^2/sr, while the maximum decreased from 28.1 nW/cm^2/sr in 2013 to 19.9 nW/cm^2/sr in 2022 (−29% overall). Trieste (Italy)–Koper maintained mean values of about 15–16 nW/cm^2/sr, showing minor annual variability within ±4% and relatively stable maximum radiance around 21 nW/cm^2/sr. Maribor recorded moderate mean values (around 14–15 nW/cm^2/sr) with an increase in minimum values in 2021 by as much as 70%, while Celje showed increase in mean values by around 6% between 2015 and 2019. Novo mesto exhibited consistently lower radiance (around 8 nW/cm^2/sr) and limited interannual variation (−2% to +5%), whereas Kranj rose gradually from 7.2 nW/cm^2/sr in 2013 to approximately 8.0 nW/cm^2/sr (+11% in 2014, −4% in 2015). Interannual mean changes rarely exceeded ±10%, indicating relatively stable or slightly increasing NTL levels consistent with urbanization, infrastructure, and economic activity across the analysed cities. Novo mesto and Kranj show the lowest radiance, with Novo mesto typically about 2 nW/cm^2/sr higher, notable deviations include a 43% drop in Novo mesto's minimum radiance in 2020 and a >70% increase in Kranj's maximum in 2021. Overall, NTL shows a gradual increase with periodic fluctuations and local anomalies, particularly in 2020 and 2022. Similar regionally diverse trends across 38 EEA countries during 2014–2022 were reported by the European Topic Centre on Human Health and the Environment under the European Environment Agency (Widmer et al. 2022).

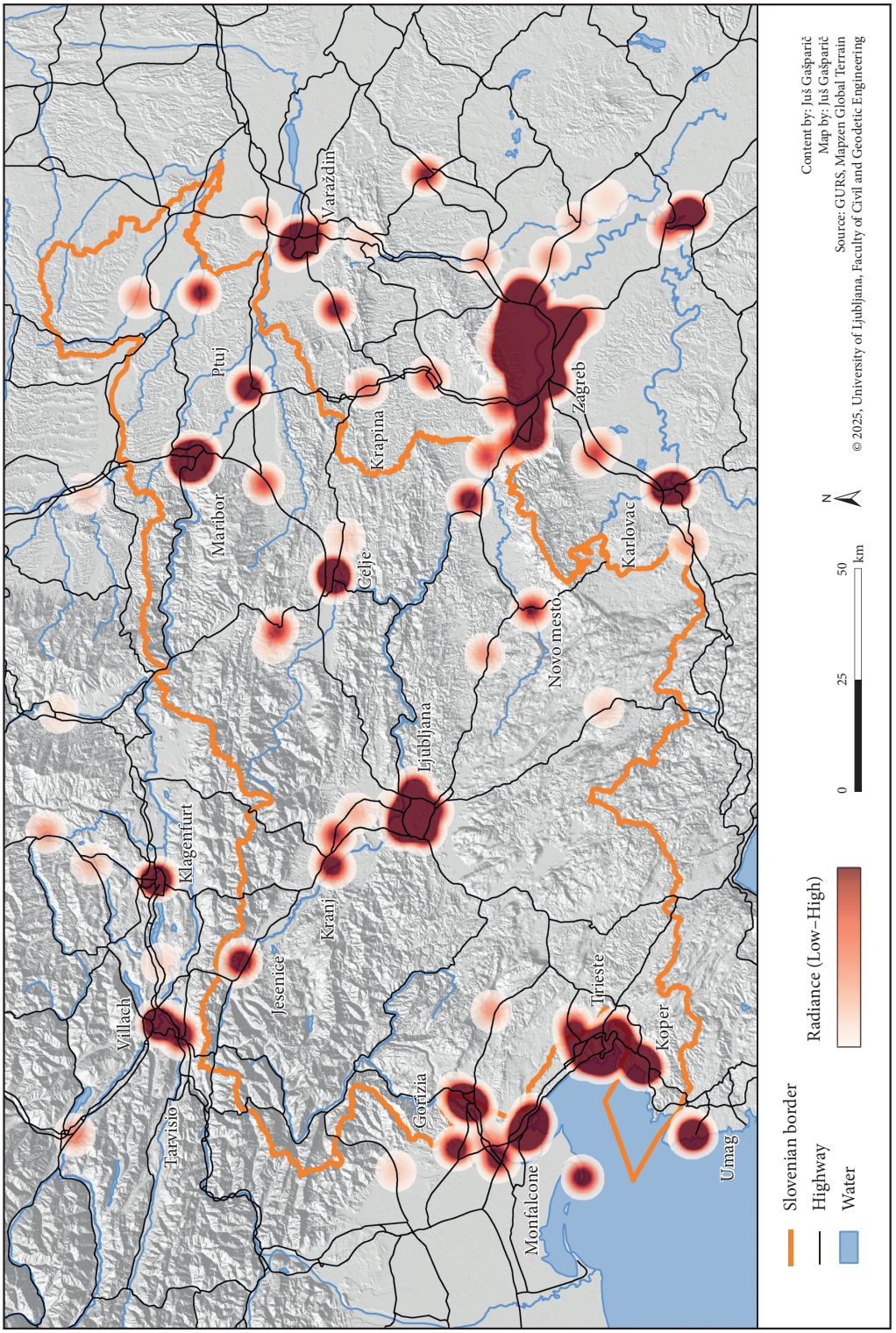
Figures 6–11 show the spatial distribution of radiance in selected Slovenian cities and Trieste (Italy), revealing a consistent pattern in which the highest NTL values concentrate in urban cores and decrease with distance. Given the coarse spatial resolution of VIIRS data, smaller individual sources of light are difficult to isolate unless they are very intense, whereas larger sources or clusters of emissions can still be

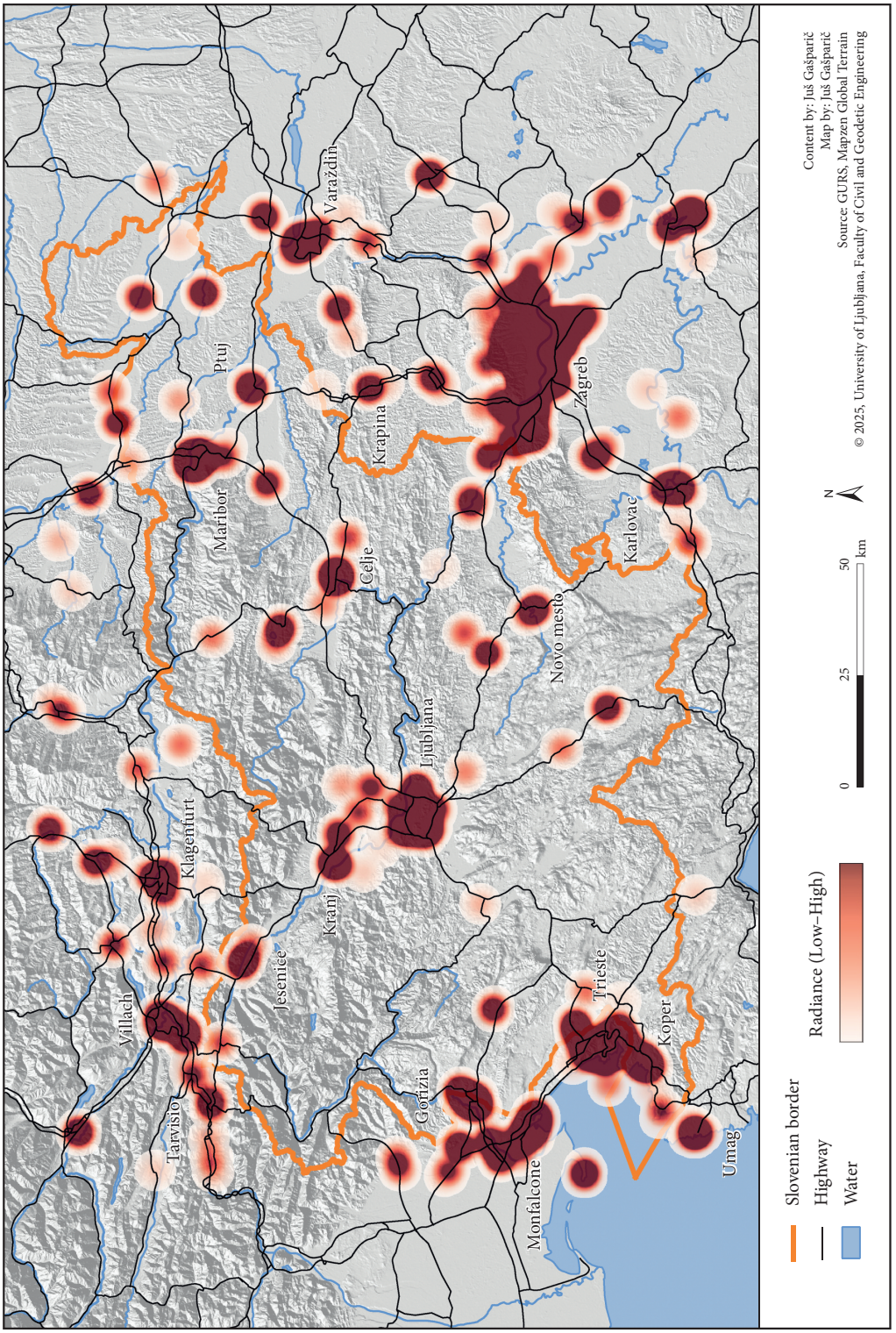
Figure 12: Change in NTL radiance (nW/cm^2/sr) in Ljubljana between 2019 and 2020. ► p. 168
Figure 13: Change in NTL radiance (nW/cm^2/sr) in Ljubljana between 2020 and 2021. ► p. 169
Figure 14: Minimum radiance values (above 20 nW/cm^2/sr) across the broader Slovenian region in 2022. ► p. 170
Figure 15: Average radiance values (above 20 nW/cm^2/sr) across the broader Slovenian region in 2022. ► p. 171
Figure 16: Maximum radiance values (above 20 nW/cm^2/sr) across the broader Slovenian region in 2022. ► p. 172


Absolute change radiance 2019/2020
1.0–1.5
1.5–2.0
2.0–2.5
>2.5
0
1
2
km
N
Content by: Juš Gašparič
Map by: Juš Gašparič
Source: NOAA, OpenTopoMap, Mapzen Global Terrain
© 2025, University of Ljubljana,
Faculty of Civil and Geodetic Engineering


Absolute change radiance 2020/2021
2.0–2.5
2.5–3.0
3.0–3.5
>3.5
0
1
2
km
N
Content by: Juš Gašparič
Map by: Juš Gašparič
Source: NOAA, OpenTopoMap, Mapzen Global Terrain
© 2025, University of Ljubljana,
Faculty of Civil and Geodetic Engineering


Slovenian border
Highway
Water
Radiance (Low–High)
0
25
50
km
N
Content by: Juš Gašparič
Map by: Juš Gašparič
Source: GURS, Mapzen Global Terrain
© 2025, University of Ljubljana, Faculty of Civil and Geodetic Engineering
Villach
Klagenfurt
Tarvisio
Jesenice
Kranj
Maribor
Ptuj
Gorizia
Ljubljana
Celje
Krapina
Varaždin
Zagreb
Novo mesto
Karlovac
Trieste
Koper
Monfalcone
Umag


Villach
Klagenfurt
Tarvisio
Jesenice
Kranj
Ljubljana
Gorizia
Monfalcone
Trieste
Koper
Umag
Maribor
Ptuj
Celje
Novo mesto
Varaždin
Krapina
Zagreb
Karlovac
Slovenian border
Highway
Water
Radiance (Low–High)
0
25
50
km
N
Content by: Iuš Gašparič
Map by: Iuš Gašparič
Source: GURS, Mapzen Global Terrain
© 2025, University of Ljubljana, Faculty of Civil and Geodetic Engineering


Villach
Tarvisio
Klagenfurt
Jesenice
Kranj
Ljubljana
Gorizia
Monfalcone
Trieste
Koper
Umag
Maribor
Ptuj
Celje
Varaždin
Krapina
Zagreb
Novo mesto
Karlovac
Slovenian border
Highway
Water
Radiance (Low–High)
0
25
50
km
N
Content by: Juš Gašparič
Map by: Juš Gašparič
Source: GURS, Mapzen Global Terrain
© 2025, University of Ljubljana, Faculty of Civil and Geodetic Engineering

recognized as broader illuminated areas. The highest radiance occurs in Ljubljana and Trieste (Italy), where urban density, transport infrastructure, and industrial areas (e.g., shopping centres in Ljubljana and ports in Trieste (Italy) and Koper) strongly influence brightness, in coastal areas emissions extend over the sea. Maribor displays high values spreading southward from the centre, shaped by major roads, the railway station, and surrounding hilly terrain where radiance declines. Celje exhibits a symmetrical and evenly distributed pattern without dominant sources, while Kranj shows comparatively low central values that decrease sharply outward, with the low minimum threshold highlighting features such as the motorway, the industrial zone near Šenčur, and Brnik Airport. Novo mesto maintains relatively low radiance despite its industrial development. Comparable spatial structures were identified in Toruń (Poland), where three zones of higher night-sky brightness contrasted with lower values farther from the city centre (Karpińska and Kunz 2019; Karpińska and Kunz 2023). Comparison with population size and road network length (Table 1) indicates a positive relationship: larger cities with more extensive road infrastructure, such as Ljubljana, exhibit higher radiance, whereas smaller centres like Novo mesto and Kranj show weaker emissions. Similar correlations between artificial light, economic activity, GDP growth, and road infrastructure development were reported by Kyba et al. (2017) and Das et al. (2021), confirming NTL as a reliable indicator of urban and infrastructural development.

During the COVID-19 pandemic (Figures 12 and 13), the largest radiance increases between 2019 and 2020 were observed within Ljubljana's ring road, intensifying toward the city centre and the Stožice Sports Centre, with notable changes also in the Šiška and Bežigrad districts, while areas such as Rudnik, Fužine, and Vrhovci showed little or no change. Compared with 2020, the strongest increases in 2021 occurred in northern Ljubljana around the Stožice Sports Centre, along the Kamnik railway line near building of the Zavarovalnica Triglav and VO-KA companies, and in the eastern industrial area near the Zalog rail yard. These patterns reflect COVID-19 pandemic containment measures, including temporary streetlight shutdowns in the city centre and rail yard, the ban on sports events in Stožice, and reduced illumination in major shopping centres. Across the entire 2013–2022 period, however, 2020 remains the only year in which NTL radiance declined consistently across all analysed cities, except Kranj, where minimum radiance increased by 20.1% (Table 6). This decrease represents a clear anomaly associated with the onset of pandemic restrictions, though within the broader decade-long variability of urban lighting dynamics in Slovenia the reductions appear temporary and did not alter the long-term trend. Comparable patterns were reported internationally using VIIRS DNB data: Xu et al. (2021) observed general NTL decreases in 20 major world cities during lockdowns, while Lan et al. (2021) showed that in China NTL changes reflected variations in human activity and policy measures rather than infection numbers. European studies reported similar declines, including about 14% in the Czech Republic (Pavlačka et al. 2023), around 50% in Polish cities (Ścieżor 2021), and up to 13% in Granada, Spain (Bustamante-Calabria et al. 2021).

According in our analyses in part 3, the minimum value map (Figure 14), radiance levels above 20 nW/cm^2/sr were detected in the largest urban centres, including Zagreb (Croatia), Trieste (Italy), Ljubljana, Maribor, and Celje, where high-intensity artificial lighting is concentrated. Other hotspots are also visible in cities such as Varaždin (Croatia), Monfalcone (Italy) and Umag (Croatia). In the average radiance map (Figure 15), the contrast between medium-sized cities and their rural surroundings becomes more pronounced. Clearly visible are smaller urban centres such as Krško and Nova Gorica (in combination with Gorizia, Italy), as well as Ptuj, Kranj, and industrial zones like Jesenice. Slightly less prominent are areas such as Velenje, Novo mesto, and Slovenska Bistrica. In the maximum radiance map (Figure 16), bright zones extend from major cities into their surrounding regions. This effect is most prominent around Zagreb (Croatia), Ljubljana and Trieste (Italy), likely reflecting patterns of urban expansion, intensive use of artificial lighting, and denser settlement structures. In addition to large cities, values exceeding the threshold are also visible in smaller centres such as Kočevje, Ajdovščina, Trebnje, Murska Sobota, Ljutomer, and Slovenj Gradec. Based on our observations, within the Ljubljana Basin, light pollution signatures are not clearly seen only in Kranj and Brnik Airport, but also in Domžale, Kamnik, and Mengeš. Similar trends are observed in neighbouring countries. In addition to major cities, light pollution can be attributed to both winter tourism (e.g., Kranjska Gora, Tarvisio in Italy, and Villach and Klagenfurt in Austria) and summer destinations (e.g., Portorož).

Weather conditions (cloud cover, snow) and natural phenomena (aurora, moonlight, wildfires) significantly influence satellite-based light pollution data. Cloud cover can increase perceived sky brightness

by reflecting light, with effects depending on urbanisation, while snow strongly amplifies brightness by reflecting all light sources, especially in already illuminated areas. Moonlight enhances surface and cloud visibility in imagery, whereas during new moon phases weather has less impact on detecting artificial light; in low-emission regions, aurora may also cause interference (Wang et al. 2022; Widmer et al. 2022). VIIRS DNB measurements are further affected by satellite viewing angle, particularly in dense urban areas where nadir observations yield higher radiance values than oblique views (Wang et al. 2022). In addition, the widespread adoption of LED lighting, which peaks in the blue spectral range (400–500 nm), lies near the lower limit of DNB spectral sensitivity (Kolláth et al. 2018). Because blue light scatters more than red or yellow light and VIIRS detectors do not respond equally across wavelengths, reduced sensitivity at shorter wavelengths means recorded values are less affected by artificial light, potentially producing overly optimistic estimates of light pollution reductions (Widmer et al. 2022; Balafoutis et al. 2025). Although satellite data indicate an annual radiance increase of about 1.8% between 2012 and 2016 (Kyba et al. 2017), these likely underestimates actual trends due to limited sensor response to modern LED spectra, and recent analyses confirm that the transition from sodium to LED lighting introduces systematic spectral bias into long-term satellite estimates (Barentine 2025). Although these limitations cannot be fully eliminated in satellite-based analyses, the use of annual composite VIIRS DNB data partly reduces the influence of short-term disturbances such as clouds, moonlight and temporary light sources. Spectral sensitivity and viewing-angle effects remain important sources of uncertainty when interpreting temporal trends.

In this study, light pollution was analysed using processed VIIRS DNB satellite data in the form of NTL composites, which provide a consistent basis for assessing the spatial and temporal extent of light pollution through heatmaps and time series. The method is less suitable for very dark areas because radiance values below 0.5 nW/cm^2/sr are set to zero in NASA's monthly and annual composites, while reflections from large glass surfaces, such as greenhouses, may locally overestimate radiance. Despite these limitations, VIIRS DNB remains the only long-term global source for light pollution monitoring and is therefore essential for informing mitigation strategies. Contrary to expectations, light pollution levels in Slovenia between 2013 and 2022 did not increase sharply, which may partly reflect the growing adoption of LED lighting and the related spectral limitations of VIIRS DNB sensors, a pattern also noted in other studies (Kyba et al. 2017; Žiberna and Ivajnšič 2018; Elvidge et al. 2022; Bhattarai and Lucieer 2024). Additional factors may include downward-facing luminaires that reduce scattering and intensity, as well as increasing public awareness of light pollution.

5 Conclusion

In this study, we conducted a detailed analysis of light pollution in Slovenia during the period 2013–2022. The findings show a slight overall increase in light pollution levels, accompanied by noticeable year-to-year fluctuations. The highest radiance values were recorded in major urban centres, particularly Ljubljana, Maribor, Celje, and the coastal area of Trieste (Italy)–Koper. In these cities, light pollution was most intense in industrial and high-traffic zones, where commercial, port, and transport infrastructures are concentrated. Time series analysis revealed that the year 2020 was a clear anomaly, showing a decrease in light pollution levels across all analysed cities, coinciding with reduced economic and traffic activity due to COVID-19 pandemic containment measures. In 2021, radiance values increased again, reaching or even exceeding pre-pandemic levels, while in 2022, a slight decline was observed in most cities. Spatial analysis with heatmaps showed that light pollution is not limited to city centres but is spreading toward suburban and peri-urban areas. The brightest zones follow major transport corridors and industrial belts, where radiance extends outward from urban cores. Mapping results for 2022 confirmed that the most illuminated areas were Ljubljana, Maribor, Celje, and the Trieste (Italy)–Koper coastal zone. Overall, the study indicates that light pollution in Slovenia did not decrease significantly between 2013 and 2022 but instead maintained a slightly increasing trend with local variations reflecting the influence of economic activity, infrastructure, and exceptional social conditions.

RESEARCH DATA: For information on the availability of research data related to the study, please visit the article webpage: https://doi.org/10.3986/AGS.14686.

6 References

Balafoutis, T., Skandali, C., Niavis, S., Doulos, L. T., Zerefos, S. C. 2025: Light pollution beyond the visible: Insights from people's perspectives. *Urban Science* 9-7. https://doi.org/10.3390/urbansci9070251

Barentine, J. 2025: Artificial light at night: State of the science 2025. *Briefing*. DarkSky International. https://doi.org/10.5281/zenodo.8071915

Barudžija, U., Ivšinović, J., Malvić, T. 2024: Selection of the value of the power distance exponent for mapping with the inverse distance weighting method: Application in subsurface porosity mapping, northern Croatia Neogene. *Geosciences* 14-6. https://doi.org/10.3390/geosciences14060155

Baynes, K. 2024: Nighttime lights. *Earthdata*. National Aeronautics and Space Administration.

Benmoshe, N. 2025: A simple solution for the inverse distance weighting interpolation (IDW) clustering problem. Sci 7-1. https://doi.org/10.3390/sci7010030

Bhattarai, D., Lucieer, A. 2024: Random forest regression: Exploring contributing factors to artificial night-time lights observed in VIIRS satellite imagery. *International Journal of Digital Earth* 17-1. https://doi.org/10.1080/17538947.2024.2324941

Bole, D. 2011: Changes in employee commuting: A comparative analysis of employee commuting to major Slovenian employment centers from 2000 to 2009. *Acta geographica Slovenica* 51-1. https://doi.org/10.3986/AGS51104

Brayley, O. D. M., Wakefield, A. 2022: The biological effects of light pollution on terrestrial and marine organisms. *International Journal of Sustainable Lighting* 24-1. https://doi.org/10.26607/ijsl.v24i1.121

Bustamante-Calabria, M., Sánchez de Miguel, A., Martín-Ruiz, S., Ortiz, J. L., Vílchez, J. M., Pelegrina, A., García, A. et al. 2021: Effects of the COVID-19 lockdown on urban light emissions: Ground and satellite comparison. *Remote Sensing* 13-2. https://doi.org/10.3390/rs13020258

Cao, C., Xiong, X., Wolfe, R., DeLuccia, F., Liu, Q., Blonski, S., Lin, G. et al. 2013: Visible/Infrared Imager Radiometer Suite (VIIRS) Sensor Data Record (SDR) User's Guide. NOAA Technical Report NESDIS 142, Version 1.1. *Technical report*. U.S. Department of Commerce, National Oceanic and Atmospheric Administration.

Chen, H., Sun, C., Xiong, X., Sarid, G., Sun, J. 2021a: SNPP VIIRS Day Night Band: Ten years of on-orbit calibration and performance. *Remote Sensing* 13-20. https://doi.org/10.3390/rs13204179

Chen, H., Xiong, X., Link, D. O., Sun, C., Chiang, K. 2020: NOAA-20 Visible Infrared Imaging Radiometer Suite day-night band on-orbit calibration and performance. *Journal of Applied Remote Sensing* 14-3. https://doi.org/10.1117/1.JRS.14.034516

Chen, Z., Yu, B., Yang, C., Zhau, Y., Yao, S., Qian, X., Wang, C. et al. 2021b: An extended time series (2000–2018) of global NPP-VIIRS-like nighttime light data from a cross-sensor calibration. *Earth System Science Data* 13-3. https://doi.org/10.5194/essd-13-889-2021

Chepesiuk, R. 2009: Missing the dark: Health effects of light pollution. *Environmental Health Perspectives* 117-1. https://doi.org/10.1289/ehp.117-a20

Das, S., Ahmed, S., Haque, S. 2021: Assessing correlation between night-time light and road infrastructure: An empirical study. In: GIScience 2021 Short Paper Proceedings. UC Santa Barbara: Center for Spatial Studies. https://doi.org/10.25436/E27P4D

Duan, J., Li, Q., Yin, Z., Zhen, S., Cao, W., Yan, S., Zhang, Y. et al. 2024: Outdoor artificial light at night and insomnia-related social media posts. *JAMA Network Open* 7-11. https://doi.org/10.1001/jamanetworkopen.2024.46156

Elvidge, C. D., Zhizhin, M., Ghosh, T., Hsu, F. C., Taneja, J. 2021: Annual time series of global VIIRS nighttime lights derived from monthly averages: 2012 to 2019. *Remote Sensing* 13-5. https://doi.org/10.3390/rs13050922

Elvidge, C. D., Zhizhin, M., Keith, D., Miller, S. D., Hsu, F. C., Ghosh, T., Anderson, S. et al. 2022: The VIIRS Day/Night Band: A flicker meter in space? *Remote Sensing* 14-6. https://doi.org/10.3390/rs14061316

Falchi, F., Cinzano, P., Duriscoe, D., Kyba, C., Elvidge, C. 2016: The new world atlas of artificial night sky brightness. *Science Advances* 2-6. https://doi.org/10.1126/sciadv.1600377

Garavito, G. A., Bennin, F., Barnett, P., Vindrola-Padros, C. 2023: What are the effects of artificial light on human health? An evidence brief. *Report*. Rapid Research Evaluation and Appraisal Lab (RREAL).

Horvat, U., Konečnik Kotnik, E., Ivajnšič, D. 2023: Svetlobna onesnaženost na Dravskem polju. In: Dravsko polje. Univerzitetna založba Univerze v Mariboru. https://doi.org/10.18690/um.ff.11.2023.8

Hügli, F. 2021: Light pollution in European protected areas: Spatial variation of light pollution in Natura 2000 sites of the Member States of the European Union. *Master's thesis*. ETH Zürich and WSL.

Kalšek, L., Budna, Ž., Hedl, A., Ravnik, J. 2021: Ocena svetlobnega onesnaženja v Mariboru, Gornji Radgoni in Senovem. *Revija za geografijo* 16-2. https://doi.org/10.18690/rg.16.2.3210

Karpińska, D., Kunz, M. 2019: Light pollution in the night sky of Toruń in the summer season. *Bulletin of Geography. Physical Geography Series* 17. https://doi.org/10.2478/bgeo-2019-0017

Karpińska, D., Kunz, M. 2023: Spatial and temporal analysis of artificial light pollution of the city night sky: A case study from Toruń. *Miscellanea Geographica* 27-3. https://doi.org/10.2478/mgrsd-2023-0015

Keck, A. 2011: NPP: Building a bridge to a new era of Earth observations. *Informational report*. National Aeronautics and Space Administration.

Kolláth, K., Tong, K. P., Kolláth, Z. 2018: Recent trends in light pollution measured from space in Hungary. In: 4th International Conference on Research, Technology and Education of Space (HSPACE2018). Hungarian Astronautical Society (MANT, Magyar Asztronautikai Társaság).

Kunz, M., Daab, D. 2024: Cartographic visualisation of light pollution measurements. *Urban Science* 8-4. https://doi.org/10.3390/urbansci8040254

Kyba, C. C. M., Kuester, T., de Miguel, A. S., Baugh, K., Jechow, A., Hölker, F., Bennie, J., Elvidge, C. D. 2017: Artificially lit surface of Earth at night increasing in radiance and extent. *Science Advances* 3-11. https://doi.org/10.1126/sciadv.1701528

Kyba, C., Altıntaş, Y. Ö., Walker, C. E., Newhouse, M. 2023: Citizen scientists report global rapid reductions in the visibility of stars from 2011 to 2022. *Science* 379-6629. https://doi.org/10.1126/science.abq7781

Lamphar, H. 2020: Spatio-temporal association of light pollution and urban sprawl using remote sensing imagery and GIS: A simple method based on Otsu's algorithm. *Journal of Quantitative Spectroscopy and Radiative Transfer* 251. https://doi.org/10.1016/j.jqsrt.2020.107060

Lan, T., Shao, G., Tang, L., Xu, Z., Zhu, W., Liu, L. et al. 2021: Quantifying spatiotemporal changes in human activities induced by the COVID-19 pandemic using daily nighttime light data. *IEEE Journal of Selected Topics in Applied Earth Observations and Remote Sensing* 14. https://doi.org/10.1109/JSTARS.2021.3060038

Li, X., Liu, S., Jendryke, M., Li, D., Wu, C. 2018: Night-time light dynamics during the Iraqi Civil War. *Remote Sensing* 10-6. https://doi.org/10.3390/rs10060858

LUC, Hoare, L. 2024: Dark skies/light impact assessment. *Methodology report*. South Oxfordshire and Vale of White Horse.

Milić, N., Đurđević, Z., Mijalković, S., Erkić, D. 2020: Identifying street hotspots using a network kernel density estimation. Revija za kriminalistiko in kriminologijo 71-4.

Nared, J., Bole, D., Breg Valjavec, M., Ciglič, R., Goluža, M., Kozina, J., Razpotnik Visković, N. et al. 2017: Central settlements in Slovenia in 2016. *Acta geographica Slovenica* 57-2. https://doi.org/10.3986/AGS.4606

Pavlačka, D., Vyvlečka, P., Barvíř, R., Rypl, O., Burian, J. 2023: Influence of COVID-19 on night-time lights in Czechia. *Journal of Maps* 19-1. https://doi.org/10.1080/17445647.2023.2235381

Perko, D., Ciglič, R., Hrvatin, M. 2021: Landscape macrotypologies and microtypologies of Slovenia. *Acta geographica Slovenica* 61-3. https://doi.org/10.3986/AGS.10384

Ravbar, M. 2011: Creative social groups in Slovenia: Contribution to geographic studying of human resources. *Acta geographica Slovenica* 51-2. https://doi.org/10.3986/AGS51204

Ścieżor, T. 2021: Effect of street lighting on the urban and rural night-time radiance and the brightness of the night sky. *Remote Sensing* 13-9. https://doi.org/10.3390/rs13091654

Sessa, C. 2021: Territorial quality of life: A case study in the cross-border area Trieste-Koper-Istria. *Futuribili – Rivista di studi sul futuro e di previsione sociale* 26-1,2. https://doi.org/10.13137/1971-0720/34414

Šumrada, R. 2005: Strukture podatkov prostorske analize. Fakulteta za gradbeništvo in geodezijo Univerze v Ljubljani.

Valinger Sluga, M., Ažman Momirski, L. 2024: Planning ports in proximity: Koper and Trieste after 1945. *Planning Perspectives* 39-2. https://doi.org/10.1080/02665433.2023.2301411

Vlaj, S. 2012: The system of local self-government in Slovenia with a special emphasis on the status of the capital city Ljubljana. *Hrvatska i komparativna javna uprava: časopis za teoriju i praksu javne uprave* 12-3.

Wallner, S., Puschnig, J., Stidl, S. 2023: The reliability of satellite-based light trends for dark sky areas in Austria. *Journal of Quantitative Spectroscopy and Radiative Transfer* 311. https://doi.org/10.1016/j.jqsrt.2023.108774

Wang, S., Li, A., Wen, K., Wu, X. 2020: Robust kernels for kernel density estimation. *Economics Letters* 191. https://doi.org/10.1016/j.econlet.2020.109138

Wang, Z., Miguel, O. R., Shrestha, R., Yao, T., Kalb, V. 2022: Black Marble User Guide (Version 1.3). *User guide*. National Aeronautics and Space Administration.

Widmer, K., Beloconi, A., Marnane, I., Vounatsou, P. 2022: Review and assessment of available information on light pollution in Europe. ETC HE Report 2022/8. *Report*. Zenodo. https://doi.org/10.5281/zenodo.7314224

Wolfe, R. E., Lin, G., Nishihama, M., Tewari, K. P., Tilton, J. C., Isaacman, A. R. 2013: Suomi NPP VIIRS prelaunch and on-orbit geometric calibration and characterization. *Journal of Geophysical Research: Atmospheres* 118-20. https://doi.org/10.1002/jgrd.50873

Wu, B., Huang, H., Wang, Y., Shi, S., Wu, J., Yu, B. 2023: Global spatial patterns between nighttime light intensity and urban building morphology. *International Journal of Applied Earth Observation and Geoinformation* 124. https://doi.org/10.1016/j.jag.2023.103495

Xu, G., Xiu, T., Li, X., Liang, X., Jiao, L. 2021: Lockdown induced night-time light dynamics during the COVID-19 epidemic in global megacities. *International Journal of Applied Earth Observation and Geoinformation* 102. https://doi.org/10.1016/j.jag.2021.102421

Žiberna, I. 2016: Svetlobna onesnaženost na območju Maribora. *Revija za geografijo* 11-2.

Žiberna, I., Gulič, J. 2020: Svetlobna onesnaženost na območju Pohorja. *Proteus* 83-2,3,4,5.

Žiberna, I., Ivajnšič, D. 2018: Daljinsko zaznavanje svetlobne onesnaženosti v Sloveniji. *Revija za geografijo* 13-1.

Žiberna, I., Konečnik Kotnik, E. 2021: Svetlobna onesnaženost v Evropi in Sloveniji. Geografija v šoli 29-3. https://doi.org/10.59132/geo/2021/3/28-38